Andrea Erazo Hidalgo

Nanochannel-based biosensing platforms to deal with infection outbreaks

Final Degree Project

Supervisor: Dra. Beatriz Prieto Simón,

Co-Supervisor: Anand Ambily Rajendran

Degree in Biomedical Engineering

UNIVERSITAT ROVIRA I VIRGILI

Tarragona

2022

Index

1 Introduction

1.1 Structure

Below are the different chapters that make up the memory of the Final Degree Project.

- Chapter 1. Introduction.
  Presents the motivation and justification of this Final Degree Project and describes the different chapters that compose it.

- Chapter 2. Theoretical framework.
  The theoretical part of the work is exposed, where the fabrication, stabilization, functionalization and characterization of porous silicon are specified. In addition to explaining its use as an electrochemical biosensor.

- Chapter 3. Methodology.
  The materials, solutions and methods that are used for the different processes that make up the development, the surface stabilization, the characterization and the validation of the membranes for their function to build electrochemical biosensors that are capable of making a label-free detection are described, presenting a shorter bacteria analysis time and simpler compared to labeled strategies.

- Chapter 4. Results and discussion.
  From the established methodology, a platform is obtained that can be used for the detection of a bacterium. The porous structure of the membrane is analyzed through SEM (Scanning Electron Microscope) images. The wettability of the membrane surface is observed at the contact angle. In the same way, after using the different functionalizations and stabilizations of the corresponding membrane, FTIR is performed to check the chemical functional groups introduced on the surface at each step of the methodology. Through Confocal Microscopy we are able to check if the membrane has been correctly functionalized and if the antibody has been immobilized in the right way. Finally, the sensitivity of the device manufactured is checked.

- Chapter 5. Conclusions.
  With all the results and discussions obtained in the previous chapters, the main conclusions are analyzed and presented.

1.2 Motivation and Justification

This document presents the work done for the Final Degree Project called "Biosensing platforms based on nanochannels to deal with outbreaks of infection" of the degree in Biomedical Engineering studied at the School of Engineering of the University Rovira i Virgili of Tarragona during the academic year 2021/22.

The project aims to generate a highly sensitive, selective, label-free and versatile electrochemical detection platform based on a pore-blockage sensing mechanism, for the early diagnosis of infectious foci. This work focuses on urinary tract infections (UTIs) developed by the bacterium *Escherichia coli* (*E. coli*). Through the assembly determined for the final sensing, which uses a macroporous silicon membrane attached to a carbon electrode, it is possible to detect and quantify the bacteria causing UTIs with the intention of preventing the development of serious kidney infections or even worst hemolytic uremic syndrome.

The work arises from the growing interest in infectious diseases that are a cause of great concern at the global health level. Nowadays a considerably important problem in public health is infections transmitted through food or ingested water contaminated with microorganisms such as bacteria, fungi, viruses or parasites. These infections, called enteric infections [1] because they specifically affect the intestine, are the cause of death of about 2 million children per year with excretion problems as the main symptom. Infections are among the top 10 causes of death worldwide [2]. Enteropathogens are a group of bacteria belonging to the Enterobacteriaceae family, which constitute a large and heterogeneous group of genetically and biochemically related bacteria. They are distributed in soil, water, vegetation and even become part of the human intestinal flora. This ubiquitous distribution means that it is inevitable that some members of the Enterobacteriaceae family will enter the food chain [3]. Strains of some known species of *E. coli* can develop bacterial UTIs [4].

As we all know, infectious diseases are defined as the presence and multiplication of a microorganism in the tissues of the host. This work will focus on the need to detect bacterial infections of the urinary tract (UTIs) because they are among the most common urinary infections. They are highly prevalent infections, UTIs present symptomatically, especially in women, between 14 and 24 years old [5]. They are characterized by the appearance of systemic symptoms such as fever, chills, malaise, nausea, vomiting and pain in the renal fossa.

UTIs usually occur because bacteria, either gram negative or positive, enter the urethra, then travel up into the bladder and cause an infection. These infections are generally caused by *E. coli*, which is part of the digestive flora and is always present in the fecal matter. Due to poorly understood mechanisms, it episodically causes disease in humans, either because it undergoes mutations that make it resistant to the control mechanisms that our body has, or because it is present in places where it should not normally be, such as the urinary tract or the same blood.

Nowadays *E. coli* infections are diagnosed by a urine sample prescribed by the primary care physician, and a rapid urine strip test [6] is used to check presence of bacteria. With this type of test one can obtain a quick but not very specific result to establish an adequate treatment. Apart from the rapid urine strip test, conventionally bacterial culture is used to identify the type of bacteria causing the infection, thus establishing a more specific diagnosis and prescribing the most appropriate antibiotic. However, bacterial culture requires qualified expertise , as well as expensive laboratory equipment and chemicals, and preparation of large volumes of medium for dilution, but the major drawback of this technique is its long analysis time.

The possibility of obtaining accurate information about the pathogen that causes infection at the test point in a shorter time is considered of utmost importance to make rapid treatment decisions, since the development of UTIs could be avoided or even prevented. Kidney infections with high severity could cause the patient to be admitted to the ICU (Intensive Care Unit). Due to this, an increase in high-quality, rapid and highly effective detection devices is needed for the detection and quantification of bacteria in the human body, in this case specifically the detection of *E. coli* [7].

Electrochemical biosensors can offer several advantages over traditional methods used for *E. coli* detection, mainly based on their rapid, highly reliable, sensitive and accurate quantitative response, cost-effectiveness and the possibility of being miniaturized. For example, an electrochemical biosensor based on an aptamer used as recognition molecule, designed "in silico" to recognize *E. coli* in aqueous matrices, was reported by L.S.W. Rocío in his PhD thesis [8]. Several electrochemical biosensors have been developed to detect bacteria and viruses, which mainly include DNA sensors, immunosensors and aptasensors. They rely heavily on the selectivity of the immobilized bioreceptor and their preparation protocols to achieve high specificity in the presence of interfering species.

Among the various materials used to develop electrochemical biosensors, porous silicon (pSi) has emerged as a promising biosensing platform due to its unique properties such as its biocompatibility, tunability of its morphological features, large surface area and versatile surface chemistry. Biosensors based on pSi have been recently reported, for e.g. the detection of MS2 bacteriophage as a model indicator of microbiological contamination, highlighting their ability to provide a highly sensitive and direct detection while overcoming matrix effects when challenged with complex samples [9]. The results showed that by tuning the morphological characteristics (i.e., pore size, and film thickness) of the pSi nanostructure, the analytical performance of the biosensor when analyzing biological samples can be significantly enhanced.

Herein we report a label-free electrochemical immunosensor using a screen printed carbon electrode (SPCE) modified with a macropSi membrane featuring arrays of macropores where bacterial binding can occur. The membrane, fabricated by a two-step electrochemical anodization process, is further functionalized either via hydrosilylation with undecylenic acid or via silanization using (3-aminopropyl)triethoxysilane (APTES) to facilitate anti-*E. coli* antibody covalent binding.

2 Theoretical framework

2.1 Nanotechnology and nanomedicine

The first time that someone talked about the idea and concept of nanoscience and nanotechnology was with a talk entitled "There's Plenty of Room at the Bottom" by physicist Richard Feynman at the American Physical Society meeting at the California Institute of Technology (CalTech) in 1959, where he described a process in which scientists would be able to manipulate and control individual atoms and molecules. Over a decade later, Professor Norio Taniguchi coined the term nanotechnology. However, it wasn't until 1981 with the development of the scanning tunneling microscope that could look at individual atoms, that modern nanotechnology began [11].

Since the introduction of the term nanotechnology, this has been an emerging area of science and technology that is leading to a new industrial revolution. Nanotechnology is a multidisciplinary scientific area based on the study, design, fabrication and synthesis of systems or devices at the atomic and molecular level; moreover, their shape and size must be at the nanometer scale, that is, they must have dimensions of around 1-100 nm, in order to obtain a fundamental understanding of phenomena and materials within that scale [12]. The understanding of the use of nanometric materials has developed new techniques and approaches aimed at improving people's quality of life in addition to more technological aspects.

The most interesting thing we can find within the field of nanotechnology is the possibility of working with materials and structures of reduced dimensions with which it is possible to obtain mechanical, chemical and biological components with much more useful and interesting properties than those of the initial volumetric material. This is partly because they possess distinct self-ordering and formation behaviors, under the control of molecular and atomic forces different from those of macroscopic objects. As a result, nanotechnology has a wide range of applications in various fields, including electronics, medicine and energy. Significant advances have now been made in the manufacture of materials of greater hardness and strength. It is known that today there are a multitude of nanotechnological products on the market, from more flexible and resistant tennis racquets to more effective and protective cosmetics [13].

The incursion of nanotechnology into the health sciences has given rise to a new scientific field called nanomedicine. The main objective of nanomedicine is to be able to develop tools to diagnose, prevent and treat diseases when they are still at an early stage or at the beginning of their development and thus determine and define or create guided procedures to deal with these critical and life-threatening clinical problems in humans. The field of nanomedicine focuses on the study of interactions between cells and/or molecules, and nanomaterials [14] at the nanoscale and makes use of devices, systems and technologies that present nanostructures capable of interacting at the molecular scale and interconnecting at the micro level to interact at the cellular level. To carry this entire field forward requires an understanding of the pathophysiological processes that influence the origin and course of a given disease.

Nowadays, there has been a progressive increase in nanomedicine to provide diagnostic and therapeutic solutions to diseases such as cancer, cardiovascular diseases, diabetes or neurodegenerative diseases (Alzheimer's disease and amyotrophic lateral sclerosis) [12]. There are currently no definitive treatments, nor effective, simple and cost-effective diagnosis for these diseases, making it necessary to create new diagnostic and therapeutic methods that are much faster, more effective and specific than those that currently exist. Nanomedicine is expected to reduce the burden associated to some of the aforementioned diseases and even provide the

capacity to regenerate organs and tissues that have been damaged. And in the near future it will even be possible to have individualized treatments at a distance, giving way to personalized telemedicine. *Table 1* shows the three different multidisciplinary areas covered by nanomedicine: nanodiagnostics, drug delivery and regenerative medicine. Their use and form may be different depending on the field for which they are intended.

Table 1. Applications of nanomedicine using nanotechnology

Nanodiagnostics	Controlled Drug Delivery	Regenerative Medicine
In vivo (diagnostic imaging): - NMR (Nuclear Magnetic Resonance) - Spectroscopy and fluorescence - Electronic tomography - Markers and contrast agents *In vitro* (nanodiagnostic devices): - Nanobiosensors - Lab-on-a-chip - Genomic and proteomic biochips	- Doxil ® (doxorubicin-loaded liposomes) - Abraxane ® (paclitaxel-loaded albumin) - Carbon nanotubes, silica particles and gold nanoparticles - Polyamidoamine	- Scaffolds - Two-dimensional nanostructured network with carbon nanotubes - Nanohydroxyapatite

Next, the three different areas covered by nanomedicine are presented. Firstly, we find the nanodiagnosis of pathologies, which consists of the development of analysis systems at the cellular or molecular level through the use of nanobiosensors, since these can detect the analytes determined with high sensitivity, based on a specific biomolecular recognition and in a fast and direct way [12]. This field also consists of the development of imaging to detect a disease or a cellular malfunction in the earliest possible stages both *in vivo* and *in vitro*.

Secondly, controlled drug delivery focuses on directing active nanosystems containing recognition elements to transport and release drugs exclusively in the affected cells or areas [15], in order to perform an adequate treatment that is effective, minimally invasive, biocompatible and with practically no side effects.

Lastly, there is the field related to regenerative medicine, which aims to replace damaged tissues and organs by applying nanotechnological tools.

In this work we will focus on the area of nanodiagnostics, specifically nanobiosensors, which are the main analytical devices being developed. Nanobiosensors are nanometric devices that are capable of detecting in real time, without or with the need of labels (e.g. fluorescent, radioactive, electroactive) and with high sensitivity and selectivity all types of chemical and biological substances. This project demonstrates the suitability of macropSi membrane-modified screen-

printed carbon electrode (SPCE) as a novel biosensing platform for the fast, sensitive and label-free detection of *E.coli*.

2.2 Porous silicon

First of all it must be said that silicon is an element of the periodic table that is found in great abundance in nature, since we can find 28% of silicon in the earth's crust [16]. It must be specified that silicon does not exist as a pure element, but rather in compound form as silicon dioxide or silicates. Silicon dioxide is the main component of sand and can also be found in the minerals that form volcanic stones.

Once we obtain the material where the silicon is in a compound state, a very specialized manufacturing process is followed to separate the silicon from the other chemical elements. For instance, silicon dioxide is purified to obtain only the silicon from which ingots will be formed, cut and polished to obtain thin sheets, better known as silicon wafers, which will be the main material for microelectronics, since they will be used to manufacture integrated electronic devices, such as computer chips, memories and transistors, but new materials can also be developed for the field of optoelectronics, chemical and biological sensors, as well as for use in biomedical devices [16]. It should be noted that recently it is one of the materials that has attracted most attention for its application in the field of biomedicine.

2.2.1 History of porous silicon

Porous silicon (pSi) was discovered accidentally by Arthur and Ingeborg Uhlir, a married couple working at Bell Laboratories in 1956. The Uhlirs were trying to develop a technique for polishing silicon using hydrofluoric acid (HF), that is, their main goal was that when the current-potential ratio is in the electropolished regime the silicon atoms are isotropically removed and thus a thinner and polished silicon wafer can be obtained. But as silicon did not dissolve uniformly as they expected, they noticed the appearance of fine holes propagating in the <100> direction of the wafer [17] and a brownish color on the wafer surface, giving rise to pSi, which, not having the desired performance, the material was forgotten.

A few decades later in the 1970s and 1980s a great deal of interest arose because the high surface area of pSi was found to be useful as a model of the crystalline silicon surface in infrared spectroscopy, for instance as a precursor for the generation of thick silicon oxide layers and also as an electrical insulator in capacitance-based chemical sensors [16].

However, it was not until the 1990s when interest in pSi and in particular its nanostructural form increased. First the founding director of the Max Planck Institute for Microstructural Physics, Ulrich Gösele identified quantum confinement effects in the absorption spectrum of pSi and about the same year Leigh Canham, of the UK Defense Research Agency, observed photoluminescence of the material emitting a visible red-orange light at room temperature [18]. The results demonstrated efficient, tunable, room-temperature light emission at energies well above the silicon bandgap.

Shortly after, in the 1990s, the discovery of the photoluminescence of pSi stimulated theoretical and experimental research on the creation of silicon-based optoelectronic devices, displays and lasers. However, the poor chemical and mechanical stability of the material and its disappointingly low electroluminescence efficiency led to a weaking interest in the mid 1990s. But it must be said

at the same time, the discovery of the material's unique characteristics such as its large surface area, current-controlled pore size, flexible surface chemistry and compatibility with silicon microfabrication technologies, inspired further research well beyond the field of optoelectronics [16]. Furthermore, today many of the fundamental chemical stability issues present in the 1990s have been overcome as the chemistry of the material has evolved, and various biomedical applications have emerged in the fields of sensors, optics and electronics.

The vast majority of published research on pSi is based on the fabrication of silicon by electrochemical etching. This process is more generally known as "anodization" and occurs when crystalline silicon is anodized in an HF-based electrolyte solution under certain anodization conditions. The final pore morphology, thickness, density and specific surface area vary over a wide range depending on the anodization conditions (electrolyte concentration, current density and applied current time), and the properties of the silicon (doping, resistivity and orientation). Therefore, by varying these parameters it is possible to fine tune the structural characteristics of pSi, which makes this material advantageous in many biomedical and electrical applications [17].

2.2.2 Features

pSi has attracted considerable attention as a sensing platform for label-free detection of a wide range of chemical and biomolecular substances [9]. Some of these advantages derived from pSi are the broad tailoring of its structural and optical properties, large surface area and established chemistry.

One property that stands out in the use of pSi is the ability to control the morphology of the pores in its formation [17]. Being able to control the pore morphology of pSi is a crucial aspect in the design of tailor-made biosensor systems where a specific target usually requires an appropriate pore size.

Table 2 summarizes the types of pSi, morphologies and applications. Note that in the literature the term 'nanoporous' is frequently used for the micropores size regime, and 'macroporous' typically refers to pore diameters close to, or in the micrometer size scale.

Table 2. Classification of pSi structures, their morphology and proposed applications.

Pore type	Silicon type	Size range	Morphology	Application
Micropores	p	< 2 nm	Sponge-like	Microfilters and microcapacitors
Mesopores	p^+, p^{++},n^+	2–50 nm	Branchy	Biosensors
Macropores	n^+, p^+, n, p	50 nm-100 μm	Tubular	Photonic material and biosensors

Figure 1 shows an image of the three types of pores that can be found.

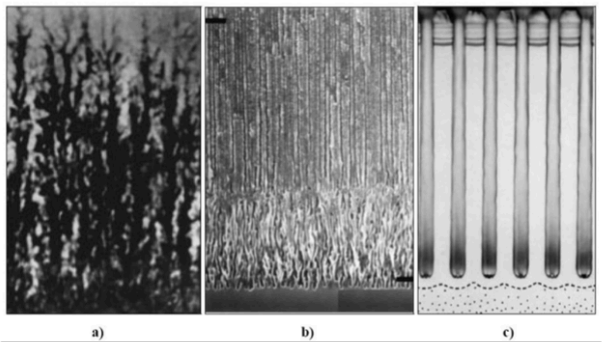

Figure 1. Photograph made by TEM and SEM of the three categories of porous silicon: a) Microporous, b) Mesoporous and c) Macroporous [19].

Pore diameters are usually selected based on the size of the biomolecule to facilitate its penetration for maximum interaction with the electric field lines in case of electrochemical biosensing [20]. It should be noted that the pore morphology of pSi can be adjusted by simply varying the etching conditions, either by varying the current density, etching time or etchant type and concentration.

Another property of pSi is its high specific surface area, reaching values around 800 m^2/g [10], providing the ability to immobilize a high density of receptors, either antibodies or DNA, within the porous matrix in a small geometric area, thus facilitating the number of receptor-target interactions. Due to its high specific surface area, the physicochemical properties of pSi are highly influenced by its chemical environment. This type of influence has allowed the development of all types of biosensors, because a high density of receptors increases the transduced signal and therefore improves the sensitivity of biosensors whether optical, electrical or chemical [21], depending on the change produced by the receptor-target interaction. Along with a fast fabrication process, pSi has a versatile surface chemistry that allows the incorporation of the desired chemical functionality into the porous material, the most commonly functionalization used are hydrosilylation or silanization reactions.

2.2.3 Fabrication

Porous silicon (pSi) can be made through different fabrication methods. However, there are some procedures that are more widely used than others due to the advantages they offer and the objective we are looking for.

2.2.3.1 Anodization

The most widely used pSi fabrication technique is anodization. This technique allows us to obtain more homogeneous pSi films, with high reproducibility and with a high control over the pore morphology.

Anodization is mainly based on an electrochemical attack or reaction on silicon wafers with an electrolyte by applying an electric field. HF is used as electrolyte because fluorine is the most electronegative element, so it has a high reductive power enough to dissolve the insulating oxide layer present on the Si surface. A twoelectrode system is used to perform the electrochemical anodization. One of the electrodes supplies electrons to the solution (the cathode) and the other withdraws electrons from the solution (the anode). In the case of pSi formation, the silicon wafer acts as the anode, and the chemical to be oxidized is the silicon itself. Moreover, a platinum wire, conductive and resistant to HF, is needed, which constitutes the cathode. The reaction that occurs at the cathode is basically the reduction of protons to hydrogen gas. These two electrodes are immersed in the electrolytic bath and a current is applied between the two electrodes through a power supply, so that the pSi film starts to form on the wafer surface [22]. Figure 2 shows a schematic of a two-electrode cell for etching silicon, with the corresponding reactions that take place throughout the electrochemical process.

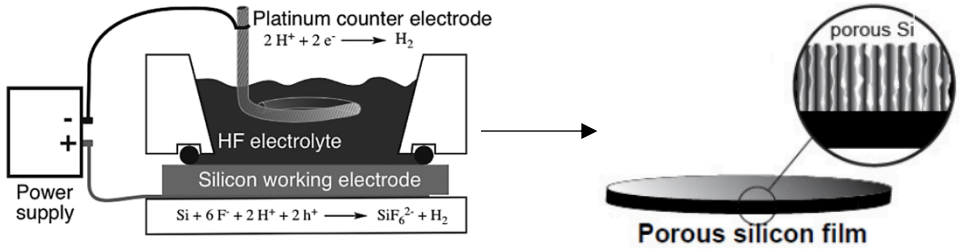

Figure 2. Scheme of the single-tank anodization cell used for fabrication of pSi. Adapted from reference [10,17]

Fabrication of pSi membrane is done using a two-step anodization procedure. First anodization is aimed at electropolishing and initializing the pore formation process using a higher HF concentration whereas the second anodization, is directed to lift-off the pSi membrane from the initial silicon wafer.

General current-voltage curve (I-V)

Part of the understanding of silicon formation can be gleaned from its I-V curve, shown in Figure 3. The curve shows characteristics common to the semiconductor/electrolyte electrochemical system: the current increases exponentially with increasing the applied potential, then increases slowly at increasingly positive potentials and then arrives to the electropolishing point. For simplicity, the I-V curves can be divided into three distinct regions: the pSi formation region, a transition region and the electropolishing regime [22].

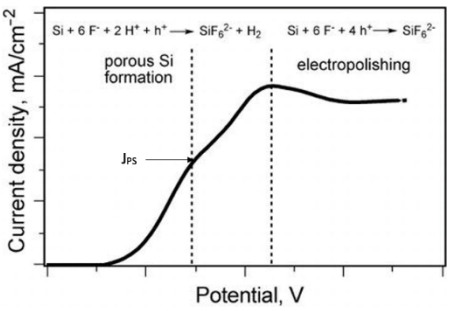

Figure 3. General current-voltage (I-V) characteristics for electrochemical etching of silicon type-p. Adapted reference [17].

The dissolution and porosification of the silicon occur under low anodic potentials passing through the silicon electrode (the anode). There is an initial exponential increase in current with applied potential that breaks down at higher potentials, showing a peak. pSi is not formed at potentials more positive than the electropolishing current (J_{PS}) [22]. The J_{PS} point divides the experimental conditions into two domains: pSi formation and electropolishing. Hydrogen evolution occurs simultaneously in the exponential regions and its rate decreases with potential, and ceases above the peak current. If the current exceeds the electropolishing threshold current, anodization results in a progressive and complete removal of silicon.

The quantitative value of the I-V curves, as well as the values corresponding to the electropolishing peak, depend on the etching parameters and the doping of the wafer. The doping refers to the type of silicon wafer used, there is n-type (phosphorus - doped) or p-type (boron - doped) (Table 2). The graph in Figure 3 shows the I-V curve corresponding to a p-type doped silicon. More information related to the I-V curve can be found in the references [23-24].

Electrochemical reactions in the chemical dissolution of silicon

We have mentioned that there are two regions on the I-V curve where anodic dissolution of silicon occurs. So the simplest reaction that occurs in the anodic dissolution of silicon in the presence of high fluorine solutions is the 4-electron oxidation, which takes place at the anode, see the equation (1). The electron holes (h+) in the valence band of silicon are used as oxidizing equivalents. The electrons provided by silicon (the anode) must be balanced by a reduction half-reaction that consumes electrons from the cathode [17]. The electrochemical process is usually the reduction of water to hydrogen gas. The product obtained in the reaction, the silicon hexafluoride ion (SiF_6^{2-}), is a stable dianion, very soluble in water and remains in solution [22].

$$Si + 6F^- + 4h^+ \rightarrow SiF_6^{2-} \quad (1)$$

However, this reaction predominates when silicon dissolution occurs under electropolishing conditions, which means that pSi is not formed. It takes place at the most positive potentials, as shown in Figure 3.

Direct dissolution of the silicon atoms and the two-valence reaction correspond to the 2-electron process, which predominates at low applied potentials. Water is spontaneously reduced by silicon, although the kinetics of the reaction is slow for silicon in its elemental state (oxidation state 0). Nevertheless, when silicon presents its +2 oxidation state, the reaction with water occurs rapidly producing the release of hydrogen and silicon in the +4 oxidation state. The 2-electron oxidation process is represented in two steps in equations 2 and 3 [22]. At low potentials, the two-electron process presented is the predominant one and, therefore, the formation of pSi is largely governed by the half-reaction presented in equation 4. Figure 4 shows the model reaction of p-type silicon (positive charge) dissolution in HF solution used.

Electrochemical step, see the equation (2):

$$Si + 2F^- + 2h^+ \rightarrow [SiF_2] \quad (2)$$

Chemical step, see the equation (3):

$$[SiF_2] + 4F^- + 2H^+ \rightarrow SiF_6^{2-} + H_2 \quad (3)$$

Net, see the equation (4):

$$Si + 6F^- + 2H^+ + 2h^+ \rightarrow SiF_6^{2-} + H_2 \quad (4)$$

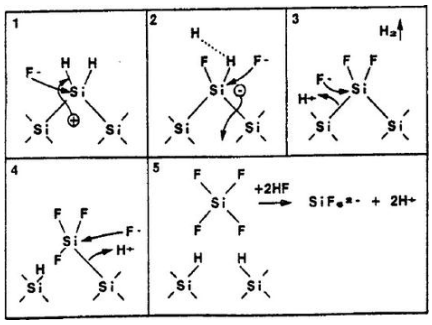

Figure 4. Reaction mechanism for the formation of porous structures in silicon [25].

Even though this simplified chemistry can explain the dissolution of silicon atoms, however, it does not explain the spatial selectivity of the reaction, which results in the formation of pores.

Formation of the porous silicon membrane

As discussed above, the anodization is performed in a two-step process. At the beginning of the first reaction to form the porous p-type silicon, the pore forms due to the electrochemical reaction with the initial HF concentration. At shallow depths, the electrochemical reaction continues to occur at the tip of the hole that is formed, because there are enough fluoride ions available to consume all the holes (Figure 5).

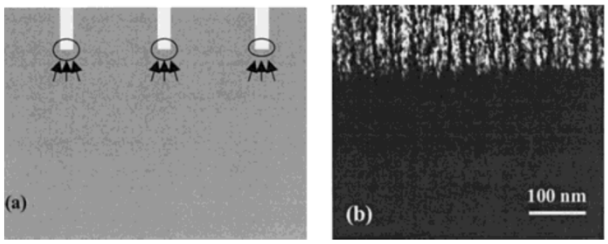

Figure 5. a) Initial stage of pSi formation, b) corresponding TEM picture [26].

As the pore depth increases, the availability of fluoride ions at the reaction point decreases. As a consequence of the high reaction rate of the pore interaction with fluoride ions, only a short time is available for the exchange of fluoride ions (active species) with the reaction by-product (inactive species). At a certain pore depth, the number of fluoride ions available is less than the number of holes available for the above-mentioned reaction. This results in the displacement of the reaction point to a slightly higher level (Figure 6).

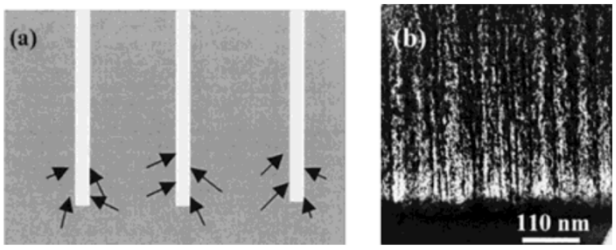

Figure 6. a) Figure showing the shift reaction to a higher level, b) corresponding TEM picture [26].

At the second anodization step is where the branching of the pores begins, resulting in the formation of a high porosity layer (Figure 7). Due to the rapid reaction, the hydrogen molecules, which as we have discussed are the by-product of the reaction, do not have time to leave and collectively exert hydrodynamic pressure on the pore walls.

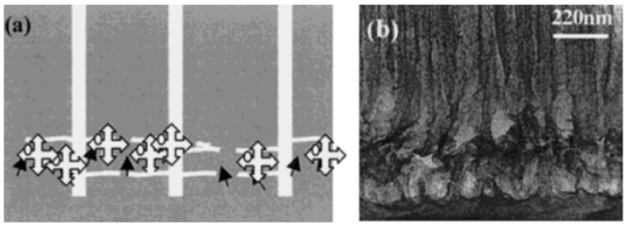

Figure 7. a) Figure showing the branching of pores and the pressure exerted by hydrogen molecules on the pore walls, b) corresponding TEM picture [26].

At some points, due to the branching of the pores, the walls become very thin and cannot withstand the hydrodynamic pressure exerted by the hydrogen molecules. This results in horizontal cracks in the layer. The presence of sufficient horizontal cracks causes the pSi film to separate from the silicon wafer. The film can then perform what is known as lift-off to produce a pSi membrane (Figure 8).

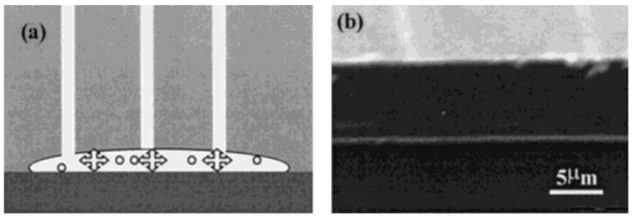

Figure 8. a) Figure showing the membrane separated from the wafer and some hydrogen molecules enclosed in the volume, b) corresponding SEM picture [26].

Finally, pSi membranes can be fabricated with different thickness by stopping the applied current for a short period just before lift-off, and reapplying the current for a short period. This gives the opportunity for the fluoride ions to diffuse to the bottom of the low porosity membrane and for the reaction by-product to leave the layer. As a result, the formation of a low porosity membrane can continue. By doing this repeatedly, any desirable thickness of the pSi membrane can be obtained and then, by applying the current for a sufficient time, the membrane can be lifted-off from the substrate. With this technique, a thickness of 70 μm can be easily obtained [26]. Pore size can also be modified through the current density, time and concentration of hydrofluoric acid that are applied on the silicon wafer in the second step of the anodization. In our case *E. coli* has a cylinder shape that measures between 1.5 to 2 μm in length, and approximately 0.5 μm in diameter, so it will be necessary to adjust the factors mentioned before to ensure the pore diameter is neither too small nor too large.

Morphology change

It has been previously mentioned that there are different parameters that control the internal morphology generated in the fabrication of pSi. These parameters will determine the characteristics of the designed structure, which are described more precisely below:

- Current density: At low current density all charge carriers are confined to a small area, hence, the pore size is small but higher current density facilitates the charge carriers to spread over a larger area around the pore tip to accommodate the increased current to minimize the interfacial impedance, therein forming larger pores. Etchant concentration or HF, along with current density applied, the concentration of etchant used can determine the porosity of pSi.

- Etching time: depending on the time used to etch the wafer, we can obtain pores with greater or lesser depth. The current density and HF concentration must also be taken into account, since these parameters are correlated at the time of obtaining the pSi.

- Silicon wafer doping: wafers can be either positively or negatively doped. Positively doped wafers are those doped with positively charged ions (holes) and negatively doped wafers are doped with negatively charged ions (electrons)[27]. In addition, the resistivity of the wafer must be taken into account, the lower the resistivity, the attacks are uniform and the layers have higher pore density.

Furthermore, these different parameters can determine other characteristics such as the speed of the attack. It has been observed that the relationship between the different parameters allows us to obtain different types of attacks so we get different pSi layers, therefore we will vary and adjust the different parameters depending on the objective of the final application that has been thought.

2.2.3.2 Other methods

In addition to anodization, alternative techniques can be used to manufacture pSi. There is a first technique called stain etching which is mainly based on chemical reactions and no additional current needs to be applied. It was reported that with this technique the growth rate of the pSi layer is proportional to the concentration of nitric acid used, while it does not dependent on the resistivity of the silicon wafer [28].The main disadvantages of this type of technique are that layers of different depths cannot be obtained, and that fabrication cannot be reproduced easily.

Secondly, photochemical etching, as its name suggests, is performed by means of intense illumination of the wafer. Although it has some disadvantages, this technique is used to manufacture small structures [13].

2.2.4 Surface stabilization

After electrochemical etching of silicon, a surface terminated with hydrogen bonds, Si-H, Si-H_2 and Si-H_3, is produced on the membrane. This freshly prepared pSi surface is very unstable, as the Si-H groups are very reactive and susceptible to be attacked by hydrolytic species in air or aqueous environments [29]. This limits its ability for further application in biomedicine. It should be said that each application will require a different chemical functionality and a different level of stability. Fortunately, the hydride-terminated surface can be easily modified with a simple

oxidation treatment, and the oxidized surface can be subsequently modified to introduce a variety of functionalities [30]. Growing a silicon oxide layer is the most common approach to stabilize and passivate the pSi surface due to its simplicity and good control over the oxide thickness [31]. Once we have an oxidized pSi surface, there are several strategies to modify the surface chemistry, but undoubtedly silanization is the most popular. The hydroxyl-terminated surface can be modified with alkyl silanes to form a layer of covalently bonded organosilanes [32]. Reactive groups at the functional end of the organosilane layer provide binding sites for biomolecule immobilization.

Apart from thermal oxidation, there are other methods to stabilize the surface of pSi, such as hydrosilylation with alkenes (e.g. undecylenic acid) or alkynes.

2.2.4.1 Thermal oxidation

The most commonly used method to stabilize the pSi surface is by thermal oxidation. Thermal oxidation is a process in which a small thin layer of SiO_2 is grown on the pSi through exposure to oxygen, which will form a barrier layer against the deposition of impurities. Si-O bonds can be created to stabilize the pSi surface and prevent rapid degradation of the membrane [13].

The thermal oxidation process is controlled by temperature, that is, by the hydrostatic pressure in the reaction chamber. Higher temperatures, around 200 °C, favor the formation of oxygen bridges between the surface silicon atoms and the second atomic layer of silicon [33]. Oxidation around this temperature also changes the surface properties from hydrophobic to hydrophilic, although most of the hydrogen atoms remain on the surface. At temperatures above 800 °C, complete oxidation of pSi occurs, where the hydrogen termination is replaced by hydroxyl groups and the thickness of the oxidized layer increases. The reaction that occurs on the pSi surface is as follows, see the equation (5):

$$Si + O_2 \rightarrow SiO_2 \quad (5)$$

In the case of oxidation outside a chamber, the following reaction can occur, see the equation (6):

$$Si + 2H_2O \rightarrow SiO_2 + 2H_2 \quad (6)$$

On the one hand, the oxidation process outside the chamber, that is, in a humid atmosphere, is much slower because of the low temperatures, which produce denser oxide. On the other hand, oxidation in the reaction chamber is faster. It should also be said that for oxide formation on pSi structures, it has been seen that the crystalline orientation of silicon influences the kinetics of SiO_2 formation [33] from a few tens of minutes to several hours.

Thermal oxidation in air allows a relatively stable oxide to be achieved, especially if the reaction is carried out at temperatures above 600 °C. The hydrophilicity of the silica layer obtained after oxidation allows the incorporation and adsorption of drugs or biomolecules within the porous structures [13].

A curious fact is that if oxidation is carried out in the presence of different ions, such as Ca^{2+}, pSi will be modified to generate a calcified form of it which is really interesting in *in vivo* applications since it is bioactive [34].

2.2.5 Functionalization

Once pSi has been stabilized, the next step requires the introduction of functional groups on the pSi surface to enable further immobilization of ssDNA, proteins, and so on.

Therefore, a further step, called functionalization, must be carried out. Functionalization is a chemical process that inserts functional groups that can facilitate the incorporation of other molecules. In this work we used membranes of macroporous silicon and two types of functionalization strategies were performed, in order to covalently bind antibodies for the detection of *E. coli*.

The first functionalization strategy tested was silanization, so after stabilization by thermal oxidation, the next step was the reaction with (3-aminopropyl)triethoxysilane (APTES). The second functionalization strategy was the hydrosilylation of pSi with undecylenic acid.

2.2.5.1 Silanization

When pSi is stabilized by thermal oxidation, the surface of the membrane shows Si-O bonds. We silanized pSi using 3-aminopropyltriethoxysilane (APTES) to introduce amino groups (NH_2) on the pSi surface. In Figure 9 we can observe the chemical reaction between APTES and the SiO bonds.

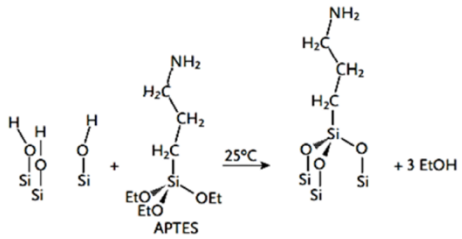

Figure 9. Silanization reaction to introduce NH_2 groups on the pSi surface [35].

Once we had the amino group on the surface of pSi it was still not viable to bind an antibody to the membrane through its amino groups. In this case, after obtaining the amino group, the membrane was subjected to succinic acid (SA) used as a linker molecule, in order to introduce carboxylic groups on the membrane surface.

Next, to activate the carboxylic groups on the surface of pSi, a reaction with 1-ethyl-3-(3-dimethylaminopropyl)carbodiimide and N-hydroxysuccinimide took place. Having the active O-acylisourea intermediate, the bacterial-specific bioreceptor (antibody), can bind the surface of pSi membrane

2.2.5.2 Hydrosilylation with undecylenic acid

The theory explains that the union between Si and carbon (C) creates covalent bonds, which are very stable bonds. In fact, Si-C bonds have a higher kinetic stability compared to Si-O bonds, this is due to the low electronegativity of C, meaning that carbon is a chemical element that attracts electrons in this case from silicon. The formation of the Si-C bond can be performed by different techniques: thermal hydrosilylation, chemical or electrochemical grafting. In this section we will focus on hydrosilylation with undecylenic acid [36].

Freshly etched macroSi membranes were placed in the reaction bottle and the air was flushed out using a vacuum pump. Nitrogen was flushed for 15 mins followed by the addition of undecylenic acid. Next, at a high temperature of about 150°C and continuous flow of nitrogen (N_2), carboxylic groups were introduced on the surface.

In order to activate the carboxyl groups, the carbodiimide activation process described above was applied, followed by antibody immobilization. In this way the surface of the pSi was prepared for the next part of the work. But before moving on to biosensing, previous characterization of both the morphology and surface chemistry of the pSi membranes was performed.

2.2.6 Characterization

Morphological characterization of pSi membrane was carried out by Scanning Electron Microscope (SEM), while Fourier Transform Infrared Spectroscopy (FTIR), Confocal Microscope and contact angle techniques were used to evaluate stabilization, functionalization and modification of pSi.

2.2.6.1 Contact angle

Contact angle is a measure of the ability of a liquid to wet the surface of a solid. In this investigation the liquid was water and the surface pSi. The shape of the water droplet on the surface depends on the surface tension of the liquid and the nature of the surface.

So depending on the inclination of the angle of the droplet, that is, where the contour merges with the bearing surface, we can determine whether the surface is hydrophobic or hydrophilic. Therefore, if the contact angle with the surface is less than 90°, it means that the surface is hydrophilic; on other hand, if the angle is greater than 90°, it means that the surface is hydrophobic (Figure 10).

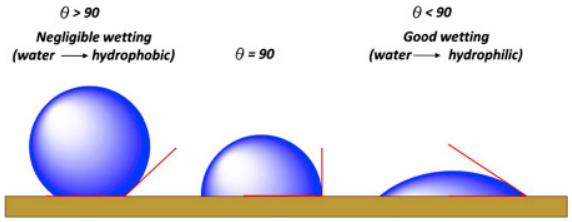

Figure 10. Contact angle measurements [37].

2.2.6.2 FTIR

Fourier Transform Infrared Spectroscopy (FTIR) is a vibrational spectroscopic technique that shows the absorption peaks corresponding to the vibration frequencies between the bonds of the atoms that make up the material to be analyzed [38]. For example, it can identify the presence of NH_2 bond after silanization with APTES on the surface of the pSi membrane through the absorption band present at a specific frequency. Therefore, since each material contains a unique combination of atoms, there are no two compounds that produce exactly the same infrared spectrum.

The advantages of this technique are that it is non-destructive, identifies unknown materials, determines the quality of the material and the quantity of components present in the material to

be analyzed [38]. In this work an analysis process was carried out in order to detect the bonds established after each modification step, to verify that the stabilization and functionalization techniques performed on the samples were correct.

2.2.6.3 Confocal Microscopy

Confocal microscopy is an optical imaging technique to increase the optical resolution and contrast of a micrograph by using a spatial hole to block out-of-focus light in the image formation. There are several applications in which the confocal microscope is used, one application is that 3D objects can be visualized by scanning several optical planes and stacking them using suitable microscopy deconvolution software [39] and it is also possible to analyze multicolor fluorescence stains using state-of-the-art confocal microscopes that include several lasers and emission/excitation filters that allow to see the functional groups present in the samples and confirm that the desired chemical groups are present as well as confirming the immobilization of antibodies or other biomolecules and so on.

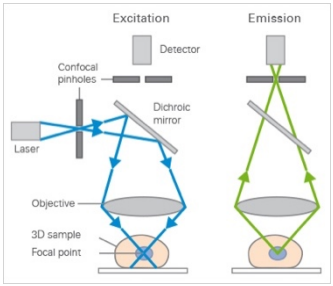

Figure 11. Excitation and emission light pathways in a basic confocal microscope configuration [39].

With this technique we can confirm if the pSi membrane surface has been properly functionalized.

2.2.6.4 SEM

Scanning Electron Microscope (SEM) is characterised by its use of an electron beam to form the image, its high resolution and its large depth of field. Due to the interaction of the electron with the material, different signals are generated that allow results to be obtained, such as the morphology or topography of the sample [40]. For this reason, we used this type of microscope to check the pore diameter and film thickness of the pSi membrane.

2.3 Biosensor

A biosensor is an analytical device that incorporates a biological element, or biomimetic, intimately associated with a physicochemical transducer, which in the presence of the analyte produces a discrete or continuous electrical signal, proportional to the amount present in the biological element [41]. A biosensor consists mainly of these parts: a bioreceptor and a transducer (Figure 12). The detection principle of a biosensor is based on the specific interaction between the analyte of interest and the bioreceptor. Thus the bioreceptor provides selectivity by its affinity towards the analyte of interest. As a result of this binding, there is a variation of one or more physicochemical properties (pH, electron transfer, heat transfer, change of potential, mass, variation of optical properties) detected by the transducer [42]. The transducer transforms the response of the recognition element into an electronic signal indicative of the presence of the

analyte under study or proportional to its concentration in the sample. The output can be in the form of a change in electrochemical properties, optical properties, and so on.

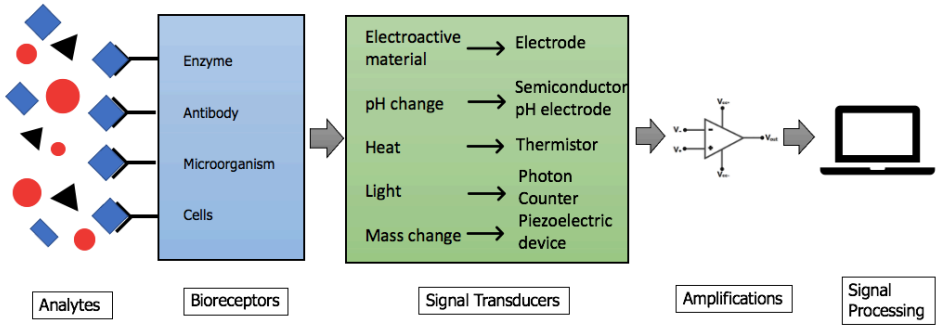

Figure 12. Scheme of a biosensor. Adapted from reference [43]

Biosensors as analytical tools should be cheap, small, easy to transport and use by non-specialised personnel, have high sensitivity and specificity, be accurate, reproducible, have a good resolution and a fast detection rate [44].

2.3.1 Classification

Biosensors can be classified according to the recognition element or the type of transducer used to convert the generated signal (Figure 13). According to their biorecognition element, biosensors can be classified as immunosensors, DNA sensors, enzymatic sensors, tissue-based sensors, and others. And according to the transduction mechanism, biosensors can also be classified as electrochemical biosensors, optical biosensors, piezoelectric biosensors, and so on.

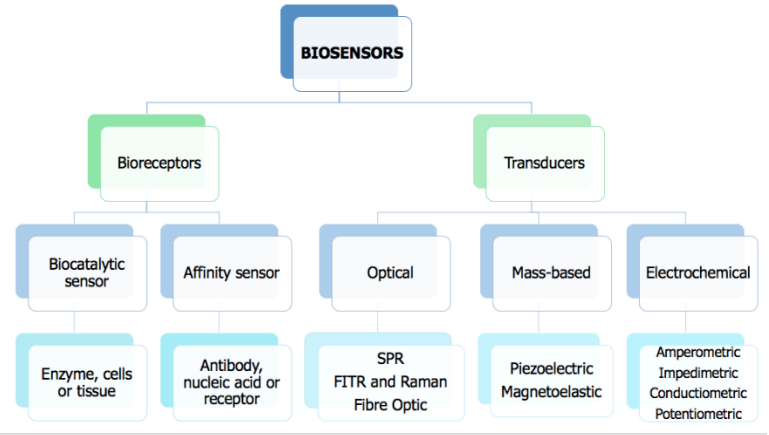

Figure 13. Classification of biosensors. Adapted from reference [43]

2.3.2 Electrochemical Biosensors

An electrochemical biosensor is a sensor with an electrochemical transducer. Electrochemical transduction is performed by a junction to a measurable current (amperometry), charge or potential accumulation (potentiometry), change in resistance (impedance) or in the conductive properties of the medium between the electrodes (conductometry) [45]. Depending on the

detection technique, electrochemical biosensors are divided into four types: amperometric/voltammetric, potentiometric, impedimetric and conductometric.

2.3.2.1 Amperometric and voltammetric biosensors

Amperometric and voltammetric techniques are based on the measurement of the current resulting from the electrochemical oxidation or reduction of an electroactive species. That is, they measure the current flowing between the working electrode (e.g. Pt, Au or C) and the auxiliary electrode, when a potential is applied in relation to the reference electrode. On the one hand, if the change in current is monitored over time at a constant potential, it is called amperometry. On the other hand, if the changes in current are measured over a set potential range, it is called voltammetry, which is useful for evaluating different electrode modification steps. Voltammetric techniques are useful for low-level quantification when the potential is applied by pulses (e.g. differential pulse voltammetry (DPV), square wave voltammetry (SWV)).

Amperometric/voltammetric biosensors focus on monitoring the changes in current due to redox reactions at the working electrode when the analyte of interest is recognized by the bioreceptor [10]. Of this section we use 3 techniques:

CV

Cyclic voltammetry (CV) is a very powerful and popular electrochemical technique commonly used to investigate the reduction and oxidation processes of a given material [46]. It is an electrochemical technique in which a certain electrical potential is applied inside an electrochemical cell to a working electrode immersed in a solution containing an electroactive species and the intensity of current flowing through this electrode is measured, generating a cyclic voltammogram. CV can be used to characterize changes on the sensor surface at each step of modification.

DPV

Differential Pulse Voltammetry (DPV) is an electrochemical technique characterised by a scalar pulse excitation signal where the base potential increases gradually in small intervals between 10 and 100 mV [47]. The pulse amplitude ΔEp is constant with reference to the base potential. It is a technique that is highly sensitive.

SWV

Square Wave Voltammetry (SWV) is a voltammetric analytical technique in which a variable amplitude gradual potential is applied to it, to which a high frequency (20-100 Hz) square wave is superimposed whose increase coincides with the beginning of the next pulse [48]. The measured current is detected twice, once for the reduction reaction and once for the oxidation reaction. Thus, the direct pulse produces a cathodic current while the reverse pulse generates an anodic current. Like DPV, this is a highly sensitive technique that can be used for quantification purposes.

2.3.2.2 Potentiometric biosensors

A potentiometric biosensor can be defined as a device incorporating a biological sensing element connected to an electrochemical potential transducer [49]. The parameter measured in the

potentiometric biosensor is the potential difference between the working electrode and the reference electrode in electrochemical devices with negligible current flow. These devices have a promising practical application, since many of these biosensors are currently available on the market, such as potentiometric biosensors with glass electrodes and metal oxides.

2.3.2.3 Impedimetric biosensors

Electrochemical impedance spectroscopy (EIS) is a widely used technique for measuring the resistive and capacitive properties of materials by using a small sinusoidally varying potential [10]. By adjusting the excitation frequency of the applied potential, complex impedance, including real impedance (resistance) and imaginary impedance (capacitance and inductance), can be calculated. Due to the ability to directly probe the interfacial properties of a modified electrode, EIS has been rapidly developed to monitor biorecognition events on the electrode surface such as biomolecular recognition events of specific binding proteins, lectins, receptors, nucleic acids, whole cells, antibodies. Many studies on impedimetric biosensors focus on immunosensors and aptasensors [50].

EIS can function as a label-free detection system, where changes in the electrical properties of the surface can be measured from the presence of the analytes of interest alone. Hence, EIS will be used to monitor the different steps during the functionalization and modification of the biosensor [43]. In addition, labels can also be introduced into impedimetric detection systems to improve sensitivity.

However, there is a major drawback of EIS, which is that there is a possibility of interaction of other substances on the electrode surface. Then, as a consequence of the high sensitivity of EIS, non-specific adsorption can have an effect on the monitored signal and thus cause interferences.

2.3.2.4 Conductometric biosensors

Conductometric biosensors can control changes in conductivity, that is, they can control the ability of a material or substance to allow electrical current to pass through upon detection of the analyte. Conductometric biosensors usually include enzymes whose charged products cause changes in ionic strength and lead to an increase in conductivity [51]. Conductometric biosensors have been widely used in different applications, such as environmental monitoring, clinical analysis and detection of food microorganisms.

2.3.3 Electrochemical biosensor based on porous silicon

pSi has demonstrated a multitude of advantages in addition to presenting great versatility in its application as biosensors. Since Sailor and co-workers [52] first reported the use of oxidized pSi as an optical biosensor for the investigation of basic biological systems until today where we find different research groups still pursuing the development of pSi-based optical biosensors during the last years [53-55] the different properties of pSi have been observed.

So pSi is a promising material for sensing applications due to the capability of pore morphological changes (such as pore size, pore depth and porosity) that can be easily adjusted by varying the parameters explained in the electrochemical anodization section (such as changing current density, etching time or HF concentration) which is the main method for pSi fabrication. Due to the ease of control of the pore morphology, in recent years it has boosted advances in the

detection of a wide range of chemical and biological analytes. In addition pSi has other very important characteristics as a biosensor such as having a large internal surface area for detection (up to 800 m^2/g) due to the presence of pores and excellent biocompatibility.

It also presents a high chemical versatility which allows to functionalize its surface in different ways (either by hydrosilylation or silanization) to introduce functional groups of interest (e.g. amino group or carboxylic group) to covalently immobilize various biomolecules that will function as bioreceptor (e.g. antibodies, enzymes, proteins or nucleic acids).

However, the use and development of pSi as electrochemical biosensors has been limited, although pSi as an electrochemical biosensor is able to offer a promising way to detect analytes of interest. By combining the right sensing mechanism and detection technique, electrochemical biosensors can be designed to provide label-free detection, which features shorter analysis time and greater simplicity than labeled strategies. These features, combined with the unique properties of nanostructured materials, are essential for the development of new biosensor platforms with improved analytical performance in terms of higher sensitivity, selectivity and detection efficiency for real applications. In particular, the use of porous nanostructured materials with nanochannel arrays, as is the case with the development of macroporous silicon, is of particular interest. Further development of these platforms may bring additional advantages. It is expected that increasing the large specific area of these materials will improve the sensitivity of the device compared to flat electrodes, because by creating nanochannels we increase the detection surface area, which also increases the amount of immobilized bioreceptors on the surface of the nanostructured material, and therefore the available binding sites (e.g. antigen-antibody binding in this work).

In addition, the fabrication of these macroporous silicon-based devices favors a detection strategy based on nanochannel blocking as a direct and label-free method to measure the interaction of the analyte and the capture probe immobilized in the channels. Thus, the design of these devices allows blocking of the nanochannels after analyte binding, preventing the diffusion of a redox probe added in solution towards the transducer surface, which can be measured electrochemically. Hence, the design of nanopores tailored to the ideal morphology of *E. coli*, combined with this label-free strategy, offers a simple and rapid detection method that could be easily adapted to point-of-care devices. In addition, pore size of nanoporous materials can be precisely controlled to facilitate their use as membrane filters for interfering compounds, thus minimizing matrix effects. Thus, pSi is a promising material for designing high-performance electrochemical platforms for portable analysis devices [56].

The following work presents a system based on a pSi membrane for the detection of *E. coli*. This bacterium is one of the main microorganisms involved in the development of infectious diseases of the urinary tract (UTIs). This bacterium belongs to the enterobacteria family and is part of the microbiota of the gastrointestinal tract of animals and humans. It has a cylinder shape with 1.5 to 2 µm in length, and approximately 0.5 µm in diameter, for this reason we use silicon macropores as detection nanostructure. A pSi membrane-based immunosensor is described that accounts for nanochannel blocking as a detection mechanism for *E. coli*. The binding of the bacteria to the capture antibody immobilized on the nanochannels causes partial blocking of the channels and thus prevents diffusion of the redox probe added in solution to the transducer surface. This causes a decrease in the oxidation current measured either by DPV or SWV.

3 Methodology

3.1 Objectives

The main objective of the present work is the development of a highly sensitive system based on a macroporous silicon membrane for the early diagnosis of urinary tract infections (UTIs) caused mainly by *E. coli* bacteria. Since the intention is to detect *E. coli*, pore diameter has to be optimized to allow the entrance of the bacteria into the porous membrane. *E. coli* measures between 1.5 to 2 μm in length, and approximately 0.5 μm in diameter.

Hence, the specific objectives to be achieved are as follows:

- Fabrication, functionalization, and chemical characterization of macroporous silicon membranes.
- Assessing the biosensing performance of the electrochemical biosensor developed based on a macroporous silicon membrane placed on a screen-printed carbon electrode (SPCE).

3.2 Biosensor preparation

The design and fabrication of macroporous silicon membranes and substrates have been largely developed in the Department of Electronic, Electrical and Automatic Engineering of the Rovira i Virgili University (URV). But it should be said that there are some steps of the sample preparation that were carried out in the area of Servei de Recursos Científics i Tècnics at the URV.

Firstly, membranes and substrates were fabricated from the electrochemical etching of the silicon wafer. Subsequently, depending on whether we wanted membranes or substrates, the time and current density of the second anodization were changed accordingly. The steps to follow to obtain a macroporous silicon membrane and proceed with the last step of biosensing are:

1. Correct and proper preparation of the silicon wafer. It includes steps such as cleaning and removal of impurities.
2. Fabrication of the pSi by 2 electrochemical attacks, taking into account what we want to obtain, membrane or substrate.
3. On the one hand, pSi can be stabilized by oxidation to then be functionalized through silanization. On the other hand, pSi can be directly stabilized and functionalized through hydrosilylation.
4. Activation of functional groups to allow immobilization of the antibody to the membrane and substrate.
5. Finally, the antibody-modified macroporous silicon membrane is integrated into the electrochemical cell to detect bacteria.

3.3 Fabrication of Macroporous Silicon

3.3.1 Set-up

The porous silicon used in this experimental part was fabricated by two electrochemical anodization steps in the presence of a basic hydrofluoric acid (HF) solution at different concentrations. The experimental setup is shown in Figure 14. The main component of the system is a customized electrochemical single-tank cell, coupled with a current source which is also capable of measuring the potential difference between the two electrodes. The system used in this part is controlled by a determinate software on the computer that controls the current density and etching time applied to the silicon wafer.

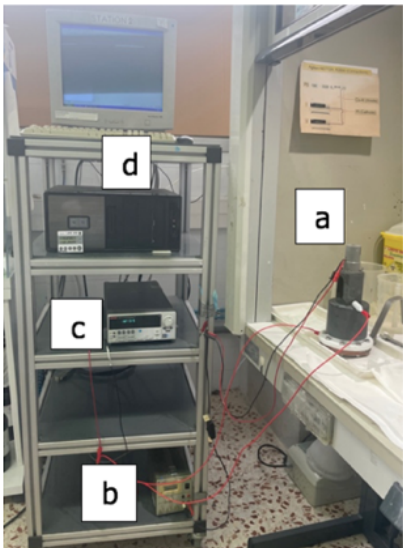

Figure 14. Photograph of the electrochemical etching set-up. a) The silicon wafer is mounted in the customized etching cell; b) coupled with a mechanical stirring system; c) the voltage-current sourcemeter Keithley 2611A applies the current and measures the resulting voltage between the electrodes; d) The system is controlled by a software run in a computer. Adapted from reference [25].

We now focus on the Electrochemical Cell. As explained in the theoretical section, we used a standard two electrode configuration: working (the silicon wafer) and counter (Pt) electrodes. Figure 15.a shows a schematic diagram of our customized electrochemical cell. The cell consists of a cylindrical polytetrafluoroethylene (PTFE or Teflon®) body designed to have on the bottom an exposed anodized area of 1.54 cm^2. This material was used because it is highly resistant to acids and organic solvents. The silicon sample is placed between the Teflon cylinder and a metal contact, with its polished side facing up and the back side in contact with an Aluminum (Al) foil. A mechanical stirring system is attached to the cell lid to facilitate the renewal of the electrolyte in contact with the silicon electrode. The metal contact on the back side is a copper disk that allows a uniform contact over the entire surface of the wafer. It should be noted that it must be

cleaned and polished to avoid any oxide film that could cause preferential current flows and thus inadequate anodization. Eight screws fix the Teflon cell and the metal contact.

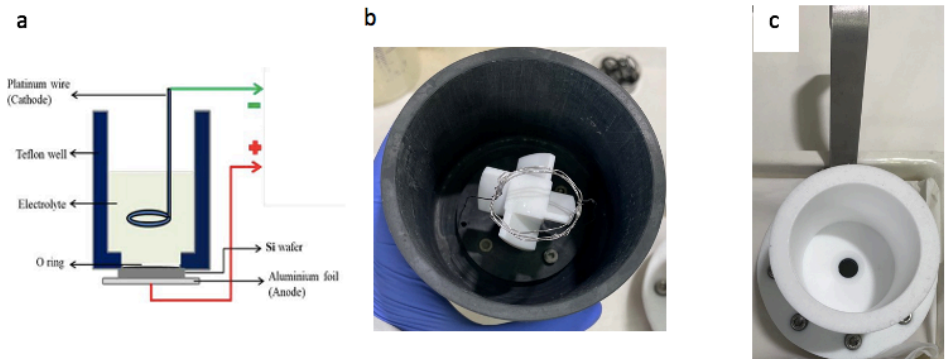

Figure 15. a) Schematic diagram of the electrochemical cell used in the pSi fabrication; b) and c) photographs of the customized cell with a view of the stirrer and the Pt electrode, and the interior of the cell body with the exposed silicon at the bottom. Adapted from reference [25].

The HF-based solution was poured into the etching cell and the cell was kept in the dark by placing a poly (vinyl chloride) (PVC) lid containing a mechanical stirrer and the platinum cathode. The reaction took place in the dark to prevent photogenerated currents from contributing to the pore formation process on the wafer. The stirring system ensured homogeneous anodization by renewing the electrolyte flow and improving the dispersion of hydrogen bubbles from the silicon surface. The rotation speed was controlled by adjusting the DC voltage applied to the motor controlled by the software.

Furthermore, the Pt cathode should be located not too close to the silicon surface, since relatively short distances lead to the formation of inhomogeneous pSi. Excessively large distances will imply increase cell height and thus a larger amount of electrolyte to be removed and higher resistance. The optimum distance of our cell was about 3 cm. Once the HF electrolyte was poured into the etch cell, we moved on to the anodizing step.

3.3.2 Preparation of solutions

As mentioned above, we use different concentrations of HF for each of the anodization steps. To prepare these solutions we mixed dimethylformamide (DMF) and HF at 48% and 40%, respectively, in 1:10 and 1:7.5 ratios. 1:7.5 (v/v) of 48% HF in DMF, and 1:10 (v/v) of 40% HF in DMF were used for the first and second step of anodization, respectively.

It has been mentioned that before performing the anodization process, the silicon wafer is subjected to a previous step in which the impurities that may be present are cleaned. For this an aqueous 5% HF solution was used.

3.3.3 Sample preparation

We used p-type silicon wafers, that is, they are positively doped and have a resistivity of 10 to 20 Ω. The degree of doping and the resistivity are inversely proportional, that is a heavily doped wafer will have a lower resistivity. We cut a 2 cm x 2 cm piece of silicon. We applied 2 minutes of washing with 5% HF and then a 3 minute wash with Milli-Q water. Afterwards we washed the

sample with water and then dried it with pressurized air. Next, we put the sample inside the electrochemical cell so that the polished part of the silicon is in contact with the O-ring and the back in contact with aluminium foil on a Cu plate.

3.3.4 Anodization

To perform the anodization of the silicon wafer we have to take into account the current source and the software that controls the electrochemical attack produced inside the electrochemical cell.

Current source and control program. The etching of the silicon wafer can be controlled potentiostatically or galvanostatically. Normally the cells operate in galvanostatic mode, so the current is the set parameter, as it ensures reproducibility reaching wide ranges of porosity and pSi layer thickness. In this work a constant current source (Keithley 2611A SourceMeter) was used for pSi etching.

A software program called TestScriptBuilder (Keithley) was previously designed to control the operation of the source for manufacturing pSi. The main parameters to be configured to carry out the anodization through the software are:

- Output file. The name of the output file, which is saved on an external USB memory stick connected to the source after anodization is completed. It is a text file including the applied current (in mA), the time (s) and the measured voltage (V).
- Current. The selected galvanostatic current (mA) that we want to apply to our sample.
- Time. The time that the current passes through the silicon electrode performing the anodization.
- Time between measurements. Time between two consecutive voltage measurements.

First Anodization. To perform the first anodization we used 1:7.5 (v/v) of 48% HF in DMF and applied a current density of 2 mA/cm^2 during 1 hour.

Second Anodization. For the second anodization we changed the solution to 1:10 (v/v) of 40% HF in DMF and applied a current density of 3 mA/cm^2 to 17 mA/cm^2 for about 10 minutes each current density (Figure 16.a) until membrane is lifted-off. pSi substrates were used in parallel for characterization purposes. To obtain a substrate (Figure 16.b) we changed the current density from 3 mA/cm^2 to 14 mA/cm^2, where each current density was applied for 10 minutes.

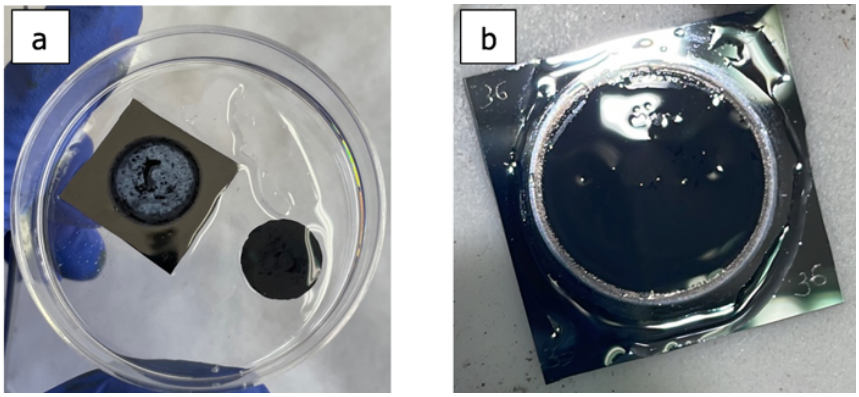

Figure 16. a) Macroporous silicon membrane; b) Macroporous silicon substrate.

3.4 Stabilization of samples

As mentioned in the theoretical section, the membranes must be oxidized in order to be able to perform the functionalization through silanization. In the case of functionalization with hydrosilylation it is not necessary to stabilize the surface of the macroporous membrane, as the same hydrosilylation provides stability to the sample. To oxidize the membrane we placed it on top of a porcelain cup, as shown in Figure 17.a, which was then placed it inside the Nonnetti oven (Figure 17.b).

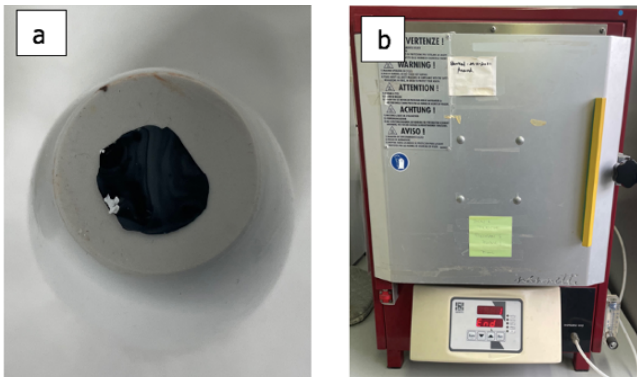

Figure 17. a) Porcelain cup; b) Nonnetti oven.

3.5 Functionalization

3.5.1 Silanization

Inside a Schlenk tube, we put a stirring bead and a maximum of 4 oxidized samples in a sample holder. We covered the Schlenk tube with a rubber stopper and fixed the tube to a shaker set at 500 rpm. In the rubber stopper we put 2 needles, the output and one for N_2 input, for 5 minutes. Then we introduced 20 mL of 99.85 % toluene with a syringe and a new needle. We let pass 10 minutes. Then we introduced 2% (v/v) in toluene of (3- aminopropyl)triethoxysilane (APTES).

We introduced 0.4 mL of APTES and wait for 1 hour. In this step amino groups were introduced on the surface of the samples. Then we removed the samples from the Schlenk tube with the sample holder and put them in a beaker that was placed in a water bath sonicator. We performed the rinsing inside the beaker, first we poured toluene for washing, and then put it back for 2 minutes in the water bath sonicator. The same step was repeated with ethanol and acetone. Finally, we dried the samples with N_2.

Then we modified the surface of the samples with succinic acid (SA). To do this, 0.2 M of SA was prepared in 16:1 (v/v) DMSO (Dimethylsulfoxide) and 0.1 M $NaHCO_3$ (sodium bicarbonate) (pH 9.4), which was later pipetted onto the sample to guarantee the presence of carboxylic group. This solution was incubated for 30 minutes. To activate the carboxylic groups 0.1 M EDC/0.4 M NHS in 0.1 M MES buffer (pH 5) was prepared. We put it on the sample and let it incubate for 1 hour.

3.5.2 Hydrosilylation

This second functionalization technique was used only with the substrates. Once freshly etched macroporous substrates were obtained, we put them in the reaction bottle separated by 2 crystals. Once the samples were in the bottle and undecylenic acid had been added, we capped the bottle with a rubber stopper. It must be taken into account that undecylenic acid is in solid state so it must be previously put in the sonicator at a temperature between 50-60 ºC, so that it becomes liquid. Then we prepared the assembly, first a silicone oil bath was placed on the hot plate to maintain a temperature of 150 ºC, and we put the reaction bottle with the samples. Once everything was ready, we took the bottle with samples in undecylenic acid and with a syringe with a needle we removed the air inside applying vacuum for 5 minutes. Then we put two needles, one for the N_2 input and the other for the output. This setup was maintained overnight. The next day samples were cleaned with ethanol and dried with N_2. With this process we introduced carboxylic groups on the surface of the substrates. To activate the functional group, 0.1 M EDC/ 0.4 M NHS in 0.1 M (pH 5) MES buffer was prepared. We put it in the sample and let it incubate for 1 hour.

3.6 Characterization

3.6.1 Morphological characterization

3.6.1.1 SEM

Once a pSi membrane was oxidised, the sample was taken to the Servei de Recursos Científics i Tècnics at the URV. SEM was used to observe whether the diameter and thickness of the pore obtained in the fabrication would be suitable for a proper detection of *E. coli*. The SEM used was a FEI Quanta 600 instrument.

3.6.2 Chemical characterization

3.6.2.1 Contact Angle

Contact angle was used to see how the surface tension of water droplets changes in contact with freshly etched, oxidised, silanised and hydrosilylated substrates. With this technique it was possible to detect directly if any chemical change occurred on the substrates before and after functionalization. The instrument used was a goniometer from Attension (Figure 18) controlled by the OneAttension software.

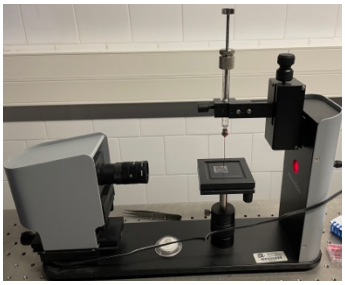

Figure 18. Attension device in the Department of Electronic, Electrical and Automatic Engineering of the URV.

3.6.2.2 FTIR

FTIR was used to see identify any chemical changes occurred in the oxidised, silanised and hydrosilylated substrates. The apparatus used to perform the FTIR was the JASCO FT/IR-6700 (Figure 19) controlled by the Spectra Manager software.

Figure 19. FT/IR-6700 in the area of Servei de Recursos Científics i Tècnics at the URV.

3.6.2.3 Confocal Microcopy

In order to verify successful introduction of proper functional groups on the substrate surface we used fluorescent dyes to label them and then characterize the cross-section of the pSi substrates via confocal microscopy. A total of 4 substrates were prepared. On the one hand, 2 substrates were silanized, and only one was modified with succinic acid and then with EDC/NHS, while the other was kept as control. On the other hand, the other 2 substrates were hydrosilylated, and again, only one substrate was EDC/NHS activated, and the other was kept as control.

The samples were then incubated in petri dishes with 10 µg/mL of Cy5-NH_2 labeled dye in 0.01 M PBS (pH 7.4) for 30 minutes, covered with aluminum foil. Amino groups form amide bonds with activated carboxylic groups. Therefore, in the results of this first protocol it was expected that the substrates with carbodiimide activated carboxylic groups show fluorescence, but in the control samples no fluorescence was expected. After 30 minutes of incubation, the samples were washed with plenty of PBS and ethanol, leaving the samples in the shaker for 30 minutes at each washing step. Then washing steps with ethanol were repeated 4 times. At the end of these 4 washes, we stored the samples in ethanol, at 4˚C overnight. The next day, before taking the samples to the microscope, we incubated the samples for 15 minutes in ethanol and repeted this process 5 times. The samples were dried with N_2. Finally confocal microscope (NIKON TE 2000-E) with dry objective (magnification 10× and numerical aperture (NA) ~0.4) was used to obtain cross-section images of the pSi samples.

3.7 Antibody Immobilization

For the immobilization of the antibody, we worked with 6 samples, 3 to be used as sensor samples and the other 3 as control samples. Triplicates are required to assess reproducibility of the experiment. All 6 samples were silanized using APTES, then reacted with SA and activated with EDC/NHS. Control samples were then incubated with 50 µg/mL of a non-specific antibody. Sensor samples were incubated with 50 µg/mL anti-*E. coli* antibody prepared in 0.01 M PBS Buffer (pH 7.4) for 2 hours. Then the samples were kept in PBS at 4˚C overnight. Finally, we blocked all the activated groups of the 6 samples with 0.01 M ethanolamine hydrochloride (pH 7.4) for 1 hour.

3.8 Biosensing

The biosensing mechanism carried out in this work is based on the partial blocking of the pores that takes place after the binding between the antibody immobilized on the surface of the pSi and the bacteria present in solution. We chose this sensing mechanism based on blocking of the pores because through different works [9] it has been demonstrated that it allows reaching a higher sensitivity than when working with flat electrodes, as any binding occurring within the pores can be sensitively detected via electrochemical means. Moreover, sensitivity is also expected to be higher due to the fact that increasing the surface of the electrode by having a porous structure, the amount of immobilized antibodies is higher, and having more bioreceptor molecules on the surface of the pSi can lead to higher signals. The partial blockage caused by analyte binding to the immobilized bioreceptor leads to a change in the oxidation current of an electroactive species (ferrocyanide to ferricyanide each 2 mM) added to the measuring solution which can be quantified by DPV or SWV.

To perform electrochemical measurements, we need an electrochemical cell (Figure 20), where we have 3 electrodes, called: Working Electrode (W) which is a screen-printed carbon electrode (SPCE), a Reference Electrode (R) which is a Ag/AgCl electrode and finally a Counter Electrode (C) which is a platinum wire that closes the electrical circuit.

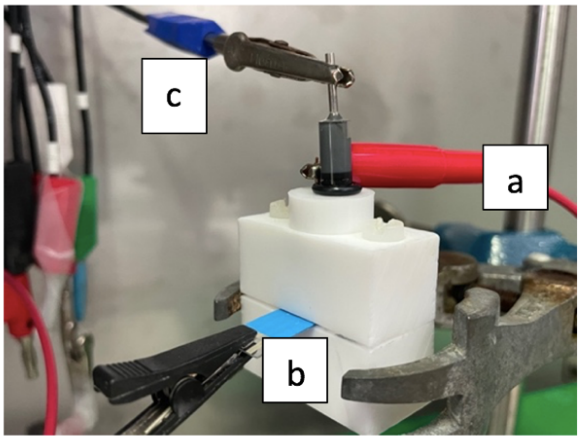

Figure 20. Cell for electrochemical biosensing. a) Counter Electrode; b) Working Electrode and c) Reference Electrode.

Before preparing the assembling of the electrochemical cell, the screen-printed carbon electrode (SPCE) must be stabilized, and thus an activation protocol was used, by applying 0.1 V for 45 s in 0.05 M carbonate buffer at pH 9.6 This process was performed as many times as necessary until the electrode response when tested via cyclic voltammetry (CV) in a 2 mM solution of ferrocyanide and ferricyanide solution prepared in 0.01 M PBS buffer at pH 7.4 was stable.

Inside the electrochemical cell, the SPCE was placed first and the membrane was placed in such a way that the side with pores of the largest diameter faced upwards and the other part towards the SPCE (Figure 21). Once the membrane and the SPCE were placed in the cell, the stabilization of the biosensing scheme was carried out by incubating the sensor in 0.01 M PBS Buffer at pH 7.4 for 30 min. Before and after incubation, a 2 mM ferrocyanide and ferricyanide solution prepared in 0.01 M PBS buffer was used as measuring solution to perform EIS, DPV and SWV measurements. 30 minutes incubation in PBS were repeated till the electrochemical measurement showed that samples were stabilized.

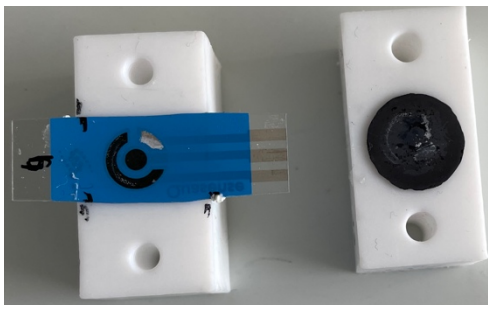

Figure 21. Components of the biosensing scheme.

As the last step, the sensing with *E. coli* was performed. Electrochemical measurements in 2 mM ferrocyanide and ferricyanide solution prepared in 0.01 M PBS buffer solution were performed before and after 30 minutes incubation of *E. coli* solutions, prepared in 0.01 M PBS at pH 7.4, in a concentration range from 10^2 cfu/mL to 10^6 cfu/mL.

4 Results and discussion

4.1 SEM

Pore size and film thickness were expected to have an effect on the electrochemical detection of *E. coli* based on pore blocking sensing mechanism. Therefore, SEM images of oxidized samples were taken to understand pore morphology and thickness. SEM images of the oxidized samples prepared applying first a current density of 2 mA/cm^2 and then a current of 3 to 17 mA/cm^2, showed an average pore diameter of 1.43 ± 0.13 µm at the top of the membrane (Figure 22.a) and 2.41± 0.36 µm at the bottom (Figure 22.b). These pore sizes were suitable to allow access of *E. coli* within the pores, and thus were chosen for the following sensing experiments. Cross-section images were taken to study the thickness of the samples (Figure 22.c). The average thickness was 81.90 ± 0.99 µm.

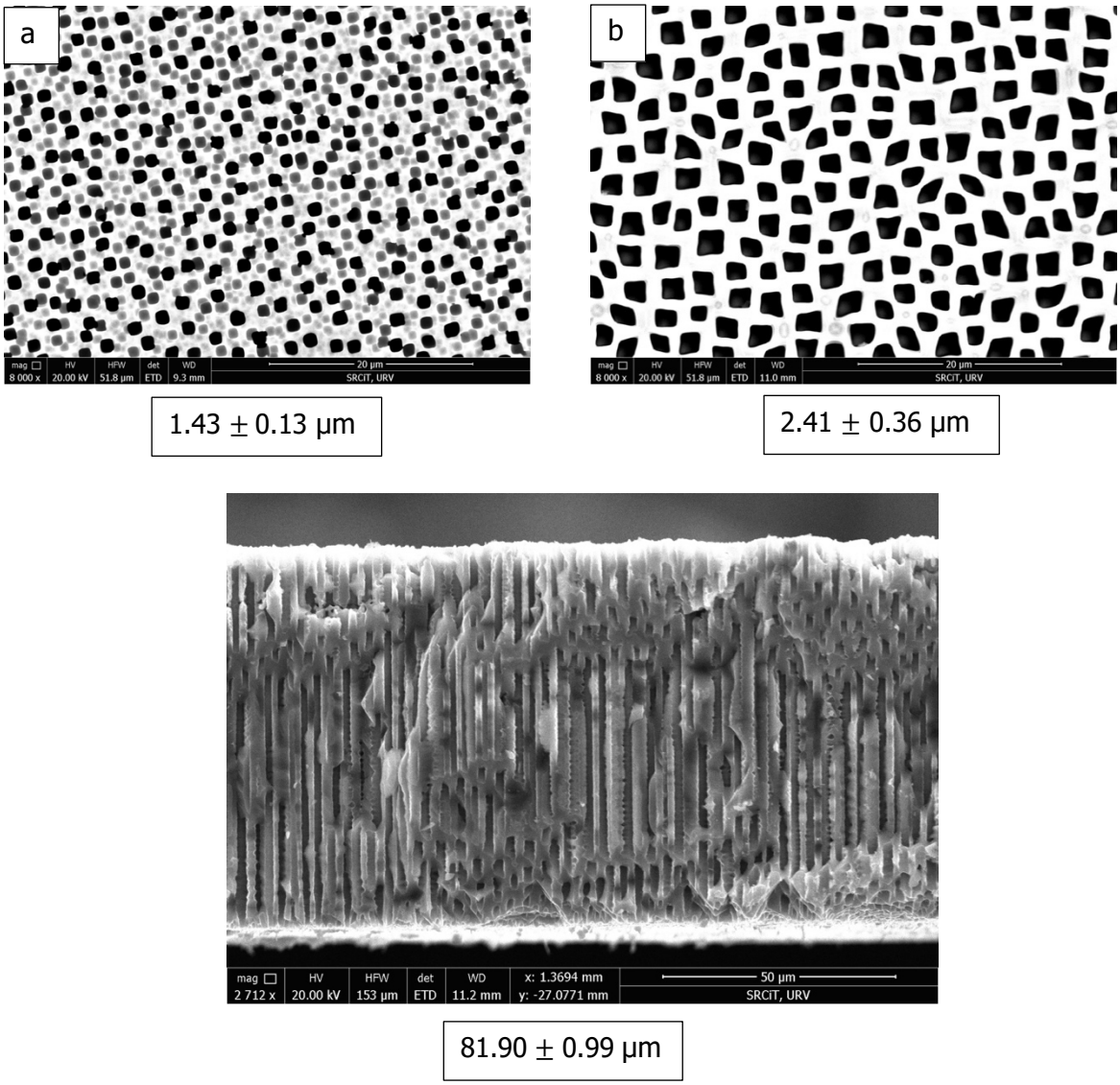

Figure 22. SEM images of macropSi corresponding to a) top view; b) bottom view; and c) cross-section.

4.2 Contact angle

Contact angle measurements provide information about the wettability of surfaces. Figure 23.a shows the contact angle of an oxidized macro-pSi sample, with reasonable hydrophilicity of 40.55 ± 2.63° Compared to oxidized sample, the one modified with APTES showed slightly higher hydrophilicity whereas the hydrosilylated sample showed reasonable hydrophobicity as shown in figure 23.b and figure 23.d respectively.

In another experiment, the contact angle of a freshly etched sample was measured, and as can be seen in Figure 23.c it showed an angle of 49.21 ± 1.35° therefore the sample was hydrophilic. Lastly, figure 23.d shows the contact angle of a hydrosilylated sample, being less hydrophilic.

These changes in wettability confirm successful functionalization of both oxidized and freshy etched pSi via silanization and hydrosilylation, respectively.

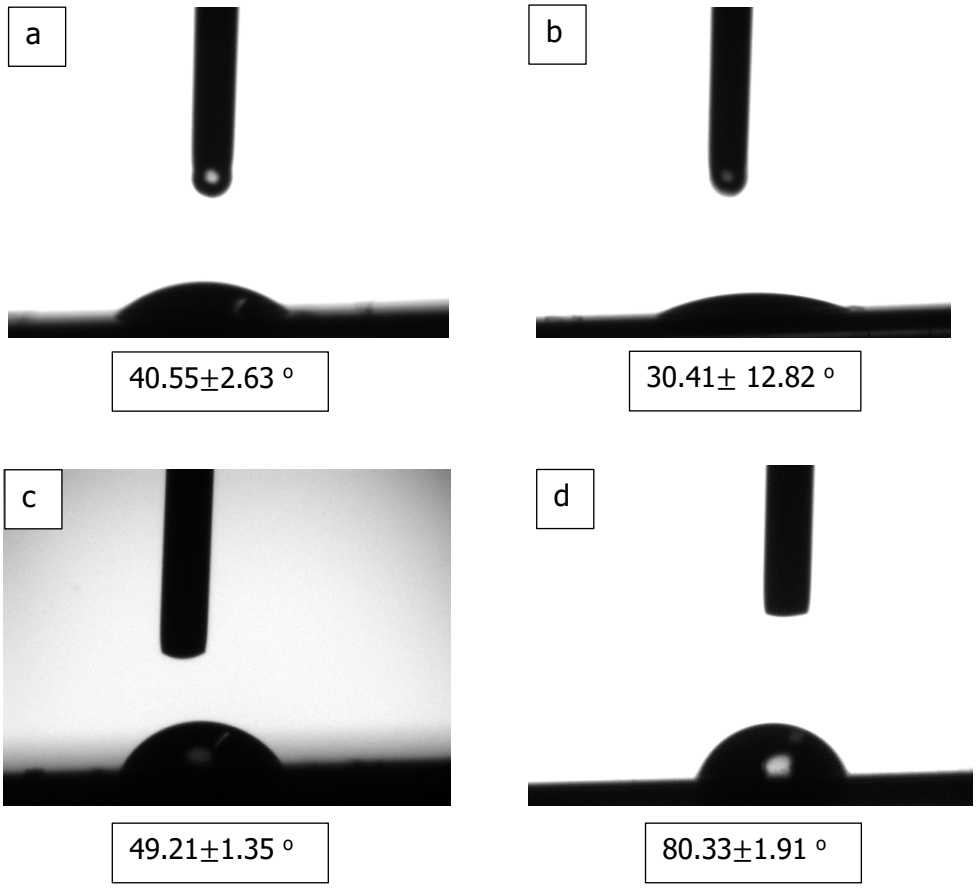

Figure 23. Contact angle for a) oxidised macroporous silicon; b) oxidized macroporous silicon modified with APTES; c) freshly etched macroporous silicon, and d) hydrosilylated macroporous silicon.

4.3 FTIR

FTIR was used to confirm that all the steps of functionalization and antibody immobilization were successful. Firstly, in Figure 24.a, the spectrum of the oxidized pSi substrate shows characteristic peaks of Si-O-Si bonds between 1000 and 1200 cm^{-1}. A OH stretching was also observed around 3100 to 3200 cm^{-1}. Secondly, in Figure 24.a and Figure 24.b we can appreciate the spectrum of pSi which has been modified through the silanization with APTES to introduce amino groups, shown by the peaks found between 1650 and 1750 cm^{-1}. Finally, we see the FTIR spectrum for hydrosilylated pSi, which shows the stretching modes of the C=O carbonyl in the region of 1650 cm^{-1}.

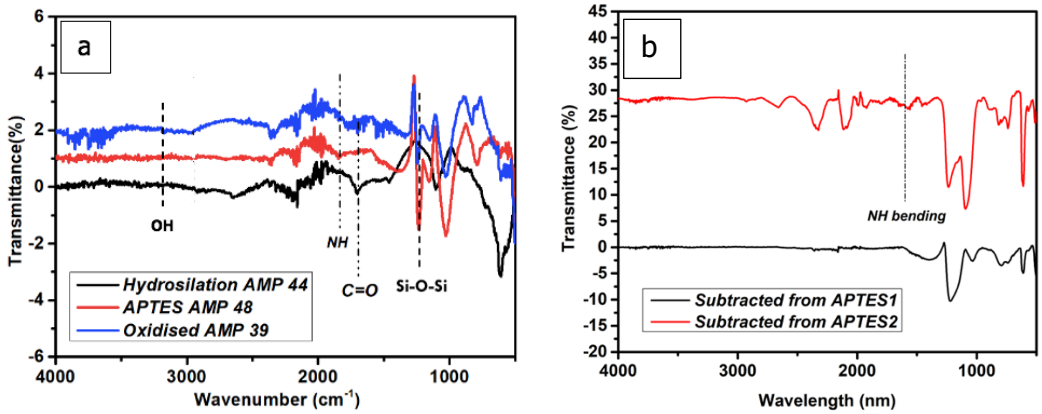

Figure 24. FTIR spectra for a) oxidised, APTES-modified and hydosilylated pSi; b) APTES-modified pSi.

4.4 Confocal microscopy

In the hydrosilylated pSi substrate was expected that only the samples with carbodiimide activated carboxylic groups could be labeled. On the one hand, we can observe that the hydrosilylated samples that were carbodiimide activated (Figure 25.a) showed fluorescence all through the thickness of the pSi film, confirming that samples were properly functionalized. On the other hand, control samples, hydrosilylated without carbodiimide activation, showed no significant fluorescence although a bit of fluorescence can be observed on the surface, that might be attributed to improper washing of the control sample with ethanol.

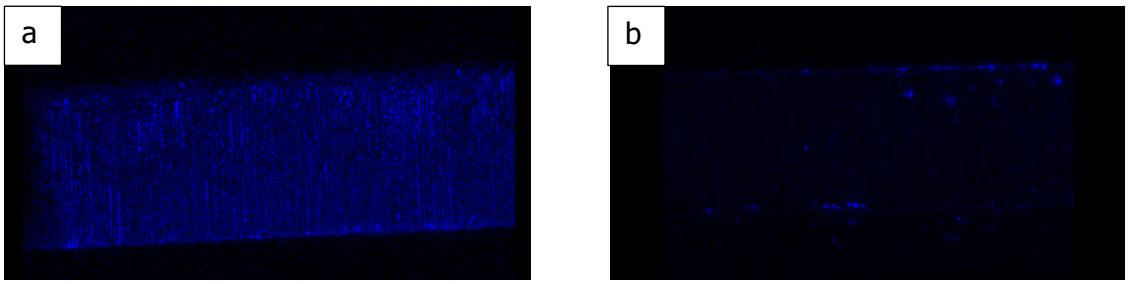

Figure 25. Confocal microscopy images from the cross-section of hydrosilylated macroporous silicon: a) carbodiimide activated b) carbodiimide not activated. The samples were incubated with 10 µg/mL of Cy5-NH_2 labeled dye in 0.01 M PBS (pH 7.4).

In figure 26.a we can observe the oxidized macroporous silicon modified with APTES samples that were carbodiimide activated showed fluorescence. And the control silanized samples after carbodiimide activation as shown in figure 26.b, did not show any fluorescence, confirming the fluorescence observed on the previous samples was not due to the non-specific adsorption of the Cy5-NH_2 labeled dye, but actually to the covalent binding of the dye with the activated carboxylic group of the substrate surface.

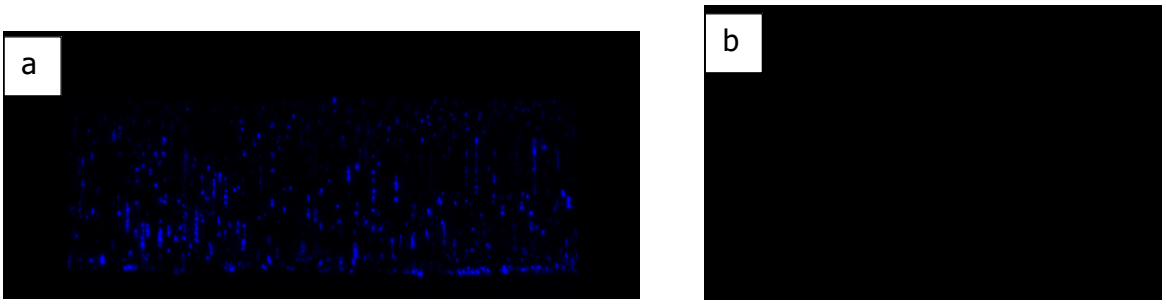

Figure 26. Confocal microscopy images from the cross-section of oxidized macroporous silicon modified with APTES: a) carbodiimide activated b) carbodiimide not activated. The samples were incubated with 10 µg/mL of Cy5-NH_2 labeled dye in 0.01 M PBS (pH 7.4).

The thickness obtained from the confocal images corresponding to the hydrosilylated samples was 102.98 $\pm$ 2.57 µm , so it is slightly larger than the thickness observed via SEM, which was 81.90 $\pm$ 0.99 µm. This may be due to the fact that substrates were used for the confocal microscopy study, while membranes were used for the SEM characterization. This study confirms the functionalization of the hydrosilylated samples was more homogeneous, pointing out this type of samples as the best option to perform biosensing studies.

4.5 Biosensing

In order to confirm the binding between the anti-*E. coli* antibody and *E. coli*, electrochemical sensing was performed using DPV and SWV measurements. For both techniques, the oxidation current of the redox probe added in solution was determined, reflecting the effect of *E. coli* binding on its diffusion through the pSi pores. To perform the sensing we used silanized samples, 3 sensors modified with anti-*E. coli* antibody, and 3 control sensors with a non-specific antibody, the latter expected to show no affinity to the target bacteria. For the detection step, *E. coli* was incubated at 3 different concentrations: 10^2 cfu/mL, 10^4 cfu/mL and 10^6 cfu/mL, on the surface of the 3 sensors and 3 controls.

DPV. Differential pulse voltammograms were obtained by sweeping the potential from -0.2 to 0.6 V in a 2 mM solution of ferrocyanide and ferricyanide prepared in 0.01 M PBS buffer at pH 7.4. Figure 27.a-c and Figure 27.d-e show differential pulse voltammograms for sensors and controls, respectively. As expected in the sensors, it is observed that increasing the concentration of the bacteria from 1 to 10^6 cfu/mL decreases the oxidation current (all the current data in Table 3).

In order to allow comparison of the immunosensors modified with anti-*E. coli* and the negative controls, modified with non-specific antibodies, current intensity values were normalized through the following formula: $\Delta I = (I_c - I_o)/I_o$, where ΔI was the normalized current change and I_o and I_c were the initial current intensity before *E. coli* incubation and current intensity after incubation of different *E. coli* concentrations. Figure 28 shows ΔI as a function of the concentration (cfu/mL) of *E. coli* to determine the sensitivity of the biosensor as the slope of the linear regression fit. The

slopes of the dose response curves for sensors and controls show that the sensitivity of the controls was smaller compared to the sensitivity shown by the biosensors modified with anti-*E. coli* antibody, confirming that the observed current changes (Figure 27.a-c) were the result of specific binding interactions between the bacteria *E. coli* and the anti-*E. coli* antibody.

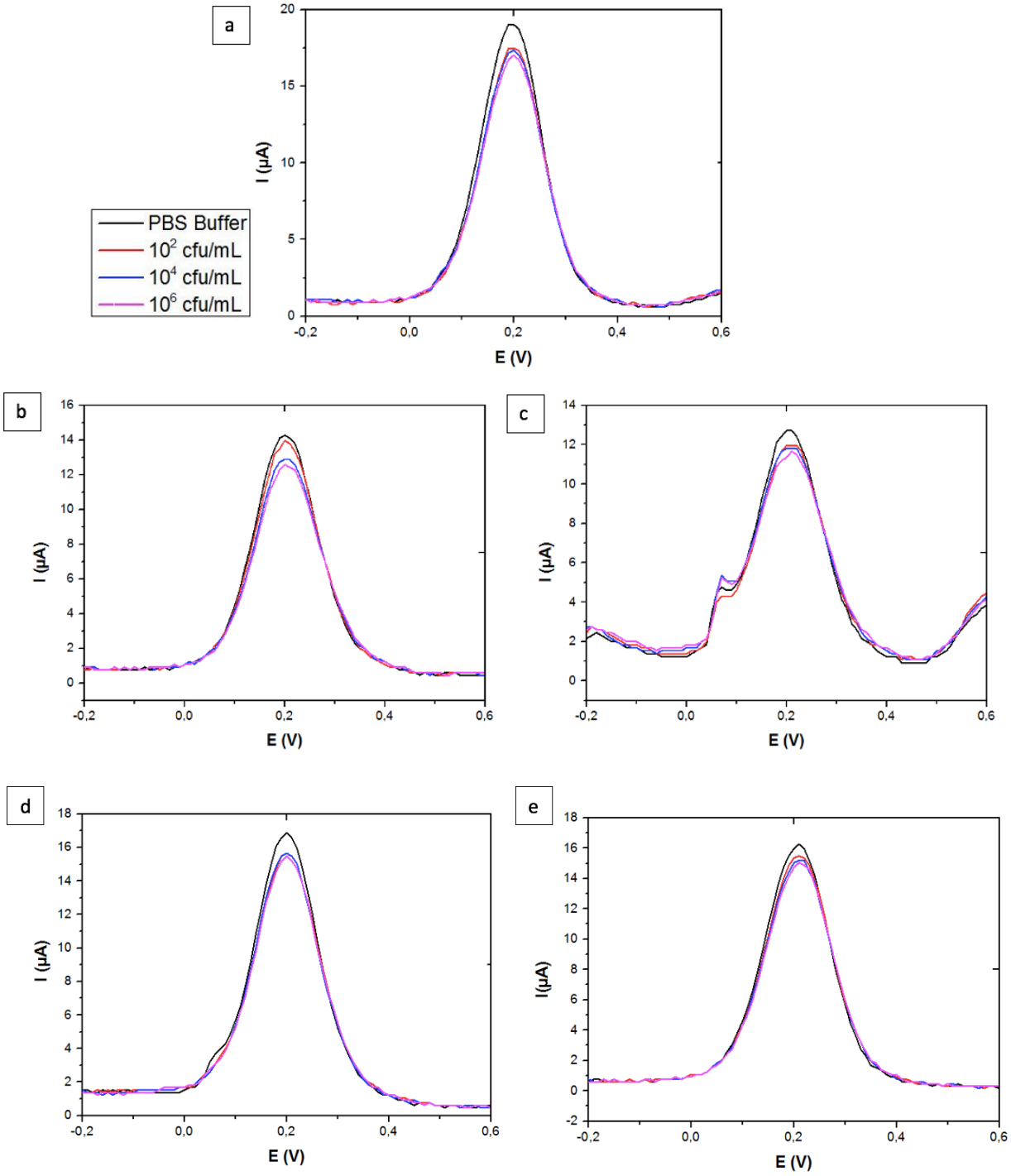

Figure 27. Differential pulse voltammograms for increasing concentrations of *E. coli* prepared in PBS incubated on a) Sensor 1; b) Sensor 2; c) Sensor 3 and d) Control 1 and e) Control 3.

Table 3. Oxidation current values extracted from the differential pulse voltammograms for each sensor and control samples shown in Figure 27.

Concentration	Sensor 1 (µA)	Sensor 2 (µA)	Sensor 3 (µA)	Control 1 (µA)	Control 3 (µA)
PBS Buffer	18.302	13.671	11.674	15.885	15.748
10^2 cfu/mL	16.865	13.214	10.778	14.655	15.040
10^4 cfu/mL	16.505	12.279	10.554	14.700	14.841
10^6 cfu/mL	16.200	11.850	10.194	14.600	14.524

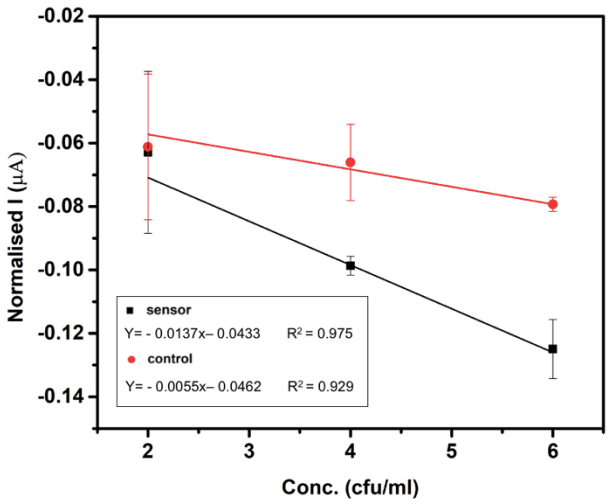

Figure 28. Dose response curves for biosensors modified with anti-*E. coli* antibodies, and control sensors modified with non-specific antibodies (control).

SWV. Measurements were also performed with another electrochemical technique, SWV to confirm the binding of *E. coli* to the antibodies immobilized on the sensor surface. Square wave voltammograms were obtained by sweeping the potential from -0.2 to 0.6 V in a 2 mM solution of ferrocyanide and ferricyanide prepared in 0.01 M PBS buffer at pH 7.4. The plots obtained by using this technique present a higher response signal than the DPV plots, so we can see the variation of current when we added different bacteria concentrations. Figure 29.a-c and Figure 29.d-e show the voltammograms obtained for sensors and controls, respectively. Meanwhile, the graphs of the control sensors with increasing concentration of *E. coli* show a slight decrease in the oxidation current after incubating 10^2 cfu/mL, but then after incubating higher concentrations, the oxidation current is practically the same (all the current parameters Table 4). With SWV technique better sensitivity can be achieved, because of the absence of the background current which indicates an interference. Moreover the current signal is the result of a difference between the experimentally measured currents.

Figure 30 plots ΔI as a function of the concentration (cfu/mL) of *E. coli* to determine immunosensor sensitivity as the slope of the linear regression fit. In Figure 30 we see that the control samples show a smaller slope, this is to say a smaller sensitivity than the biosensors with the anti-*E. coli* antibody, although in this case we have not established linear regression. Thus,

the biosensors with the specific antibody confirm that the observed current changes (Figure 29.a-c) were the result of specific binding interactions between the bacteria and the anti-*E. coli* antibody.

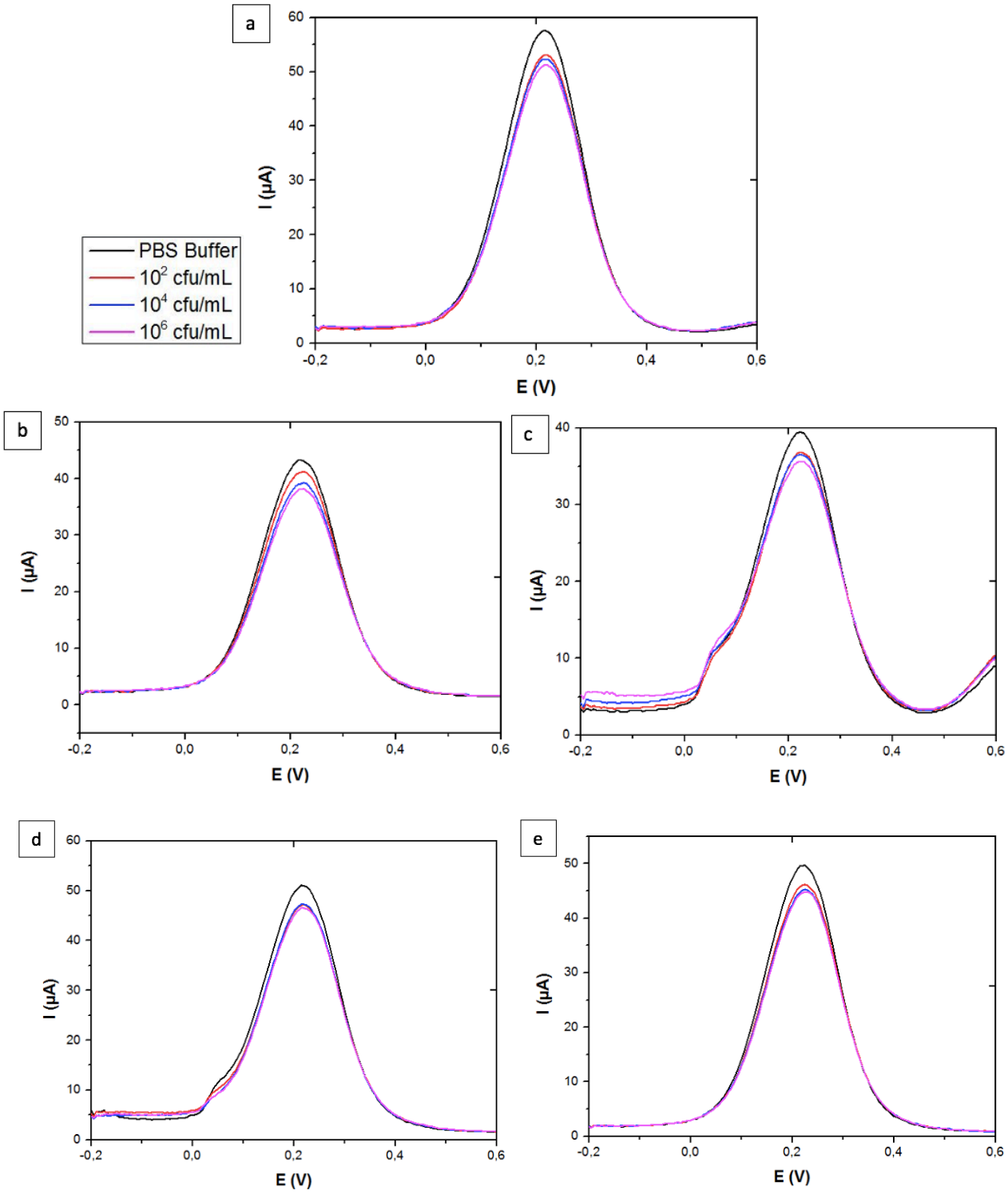

Figure 29. Square wave voltammograms for increasing concentrations of *E. coli* prepared in PBS incubated on a) Sensor 1; b) Sensor 2; c) Sensor 3 and d) Control 1 and e) Control 3.

Table 4. Oxidation current values extracted from the square wave voltammograms for each sensor and control samples shown in Figure 29

Concentration	Sensor 1 (µA)	Sensor 2 (µA)	Sensor 3 (µA)	Control 1 (µA)	Control 3 (µA)
PBS Buffer	55.244	41.426	32.177	48.052	48.317
10^2 cfu/mL	50.650	39.292	32.695	43.796	44.893
10^4 cfu/mL	49.830	37.305	29.520	43.990	43.949
10^6 cfu/mL	48.610	36.160	27.250	43.132	43.420

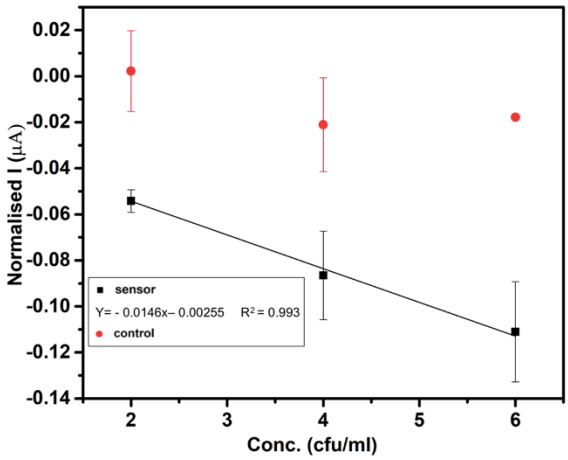

Figure 30. Dose response curves for biosensors modified with anti-*E. coli* antibodies, and control sensors modified with non-specific antibodies (control).

5 Conclusions

In this final degree project, we have developed an electrochemical biosensor based on pSi that specifically detects *E. coli* bacteria. After completing all the manufacturing and biosensing steps, it is expected that the detection platform will allow future confirmation of urinary tract infections caused mainly by *E. coli* by detecting this bacterium. The present analytical device consisted in the fabrication of macroporous silicon by means of two electrochemical attacks created by HF at different concentrations, where the first etching was performed to start the formation of the pores and the second to obtain a membrane by lift-off. Freshly etched pSi is not stable, so a stabilization step was carried out based on the oxidation of the pSi surface, then followed by functionalization. The pSi was functionalized through either silanization with APTES or hydrosilylation with undecylenic acid. It was possible to confirm the introduction of the functional groups on the surface of the samples by FTIR. Upon labeling the functionalized surface with a fluorescent dye, confocal microscopy confirmed successful functionalization through the whole thickness of the pSi film. Also the confocal studies showed that the samples functionalized using APTES showed no fluorescence in it's control sample and that's why we chose APTES modified over hydrosilylated ones. So to perform the biosensing we used silanized membranes and immobilized the anti-*E. coli* antibody. Preliminary results confirm the developed biosensor can detect *E. coli* by measuring electrochemically the partial pore blockage caused after *E. coli* binds to the immobilized antibodies on the pSi surface.

To sum up, the electrochemical biosensor based on pSi can provide a label-free detection method based on pore blocking suitable for point-of-care devices. In addition, the development of platforms for the detection of *E. coli* bacteria can help to detect early stage infections such as urinary tract and prevent the development of more serious diseases of the patient.

6 References

[1] C. Baylis, M. Uyttendaele, H. Joosten and A. Davies, "*The Enterobacteriaceae and their significance to the food industry*". Report Commissioned by the ILSI Europe Emerging Microbiological Issues Task Force. 2011.

[2] World Health Organization. (2021, December 8). *Las 10 principales causas de defunción*. (n.d.). [Online]. Available: https://www.who.int/es/news-room/fact-sheets/detail/the-top-10-causes-of-death

[3] M. T. Vazquez-Pertejo. (2021, December 9). *Diagnóstico de las enfermedades infecciosas - Infecciones - Manual MSD versión para público general*. (n.d.). [Online]. Available: https://www.msdmanuals.com/es-es/hogar/infecciones/diagn%C3%B3stico-de-las-enfermedades-infecciosas/diagn%C3%B3stico-de-las-enfermedades-infecciosas

[4] (2021, December 9). Urinary Tract Infection. Antibiotic Use. CDC. (n.d.). [Online]. Available: https://www.cdc.gov/antibiotic-use/uti.html

[5] M. Baldeyrou and P. Tattevin, "Infecciones urinarias," *EMC - Tratado Med.*, vol. 22, no. 2, pp. 1–8, 2018.

[6] (2021, January 2). Análisis de orina mediante tiras reactivas: técnica e interpretación de resultados - Revista Electrónica de Portales Medicos.com. (n.d.). [Online]. Available https://www.revista-portalesmedicos.com/revista-medica/analisis-de-orina-mediante-tiras-reactivas-tecnica-e-interpretacion-de-resultados/

[7] V. F. Ferrer, T. P. Suñé, A. A. Huerta. (2021, December 10). *Escherichia Coli*. Hospital Vall d'Hebron. [Online]. Available: https://hospital.vallhebron.com/es/asistencia/enfermedades/infeccion-por-escherichia-coli

[8] L. S. W. Rocío. (2022, January 10). Evaluación del Aptámero Diseñado "in silico" para la Detección Electroquímica de Escherichia Coli O157:H7 en Matrices Acuosas. [Online]. Available: https://repositorio.udes.edu.co/bitstream/001/5527/1/Evaluaci%C3%B3ndelApt%C3%A1meroDise%C3%B1ado%E2%80%9Cin%20silico%E2%80%9DparalaDetecci%C3%B3nElectroqu%C3%ADmicadeEscherichiacoliO157H7enMatricesAcuosas.pdf .

[9] N. Reta, A. Michelmore, C. Saint, B. Prieto-Simón, and N. H. Voelcker, "Porous silicon membrane-modified electrodes for label-free voltammetric detection of MS2 bacteriophage," *Biosens. Bioelectron.*, vol. 80, pp. 47–53, 2016.

[10] K. Guo *et al.*, "Porous Silicon Nanostructures as Effective Faradaic Electrochemical Sensing Platforms," Adv. Funct. Mater., vol. 29, no. 24, pp. 1–12, 2019.

[11] (2022, January 15). *What Is Nanotechnology*. National Nanotechnology Initiative.[Online]. Available: https://www.nano.gov/nanotech-101/what/definition

[12] L. M. Lechuga. (2022, January 20). Nanomedicina: aplicacion de la nanotecnologia en la salud. Grup. Nanobiosensores y Apl. Bioanalíticas Cent. Investig. en Nanociencia y Nanotecnología Cons. Super. Investig. Científicas, p. 15, 2005, [Online]. Available: http://digital.csic.es/bitstream/10261/44635/1/7_Nanomedicina.pdf

[13] P. Balguer. (2022, January 22). "Desarrollo de nanopartículas de silicio poroso para aplicaciones de carga-liberación de medicamentos," 2020. [Online]. Available: https://riunet.upv.es/bitstream/handle/10251/174466/Balaguer%20-%20Desarrollo%20de%20nanoparticulas%20de%20silicio%20poroso%20para%20aplicaciones%20de%20carga-liberacion%20d....pdf?sequence=1

[14] K. Riehemann, S.W. Schneider, T.A. Luger, B. Godin, M. Ferrari, H. Fuchs, "*Nanomedicine challenge and perspectives*". Angew Chem Int Ed Engl. 2009; 48(5): 872-897.

[15] F.R. González, G. G. Salgado, H. Juárez, E. Rosendo, T. Díaz, M. Paucio, C. Morales, F. Nieto. (2022, February 4). "*El silicio poroso*". Conacyt. [Online]. Available: https://www.cyd.conacyt.gob.mx/?p=articulo&id=107#

[16] S. K. Saxena, R. Nyodu, S. Kumar, and V. K. Maurya, "*Current Advances in Nanotechnology and Medicine*," in NanoBioMedicine, S. K. Saxena and S. M. P. Khurana, Eds. Singapore: Springer Singapore, pp. 3–16, 2020.

[17] M. J. Sailor, "*Nanomaterials for the Life Sciences Ceramics Science and Technology Ceramics Science and Technology Ceramics Science and Technology Advanced Ceramics and Future Materials"*. 2012.

[18] L.T. Canham, "*Silicon quantum wire array fabrication by electrochemical and chemical dissolution of wafers*", Appl. Phys. Lett. 57, 1990,1046-1048.

[19] P. F. De Carrera, R. P. Urbano, Á. R. Martínez, "*Fabricación y caracterización de supercondensadores basados en microestructuras 2d de silicio poroso".* Grupo de Micro y Nano. 2013.

[20] C. Roychaudhuri, "*A review on porous silicon based electrochemical biosensors: Beyond surface area enhancement factor*," Sensors Actuators*, B Chem.*, vol. 210, pp. 310–323, 2015, doi: 10.1016/j.snb. 2014.

[21] G. Recio Sánchez. (2022, February 22). "Aplicaciones fotónicas y biomédicas de silicio poroso nanoestructurado," Univ. Autónoma Madrid (UAM), vol. 1, no. 1, p. 212, 2013, [Online]. Available: https://repositorio.uam.es/handle/10486/14120

[22] M.A. Martín, *"Silicon Dioxide Microstrucutres Base on Macroporous Silicon for Biomedical Applications"*. 2014.

[23] V. Lehman, "*The Semiconducot-Electrolyte Junction"*, in Electrochemistry of Silicon. Wiley-VCH Verlag FmbH. p. 39-48. 2002.

[24] M. J. Sailor, "*Porous Silicon in practice: preparation, characterization and applications".* John Wiley & Sons. 2012.

[25] D. M. Knotter and T. J. J. (Dee) Denteneer, "*Etching Mechanism of Silicon Nitride in HF-Based Solutions*," J. Electrochem*. Soc.*, vol. 148, no. 3, p. F43, 2001.

[26] C. S. Solanki, R. R. Bilyalov, H. Bender, and J. Poortmans, "*New approach for the formation and separation of a thin porous silicon layer*", *Phys. Status Solidi Appl. Res.*, vol. 182, no. 1, pp. 97–101, 2000.

[27] D. Martín Sánchez, *"Desarrollo de biosensores fotónicos basados en membranas de silicio poroso"*, Tesis doct., 2019.

[28] É. Vázsonyi *et al.*, "Porous silicon formation by stain etching", Thin Solid Films, vol. 388, no. 1–2, pp. 295–302, 2001.

[29] C. Steinem, A. Janshoff, V. S. Y. Lin, N. H. Vöelcker, and M. Reza Ghadiri, "*DNA hybridization-enhanced porous silicon corrosion: mechanistic investigaitons and prospect for optical interferometric biosensing".* Tetrahedron. p. 11259-11265. 2004.

[30] J. J. Gooding and S. Ciampi, "*Dual Silane Surfsce Functionalization for the Selective Attachment of Human Neuronal Cells to porous Silicon",* Langmuir. p. 1268. 2011.

[31] J. Riijonen, M. Salomäki, J. Van Wonderen, M. Kemell, W. Xu, O. Korhonen, M. Ritala, F. MacMillan, J.Salonen and V. P. Lehto, "*Surface Chemistry, Reactivity, and Pore Structure of Porous Silicon Oxidized by Various Methods",* Langmuir. p. 10573. 2012.

[32] V. Biju, "*Chemical modifications and bioconjugate reactions of nanomaterials for sensing, imaging, drug delivery and therapy",* Chemcial Soiety Reviews. p. 744-764. 2014.

[33] R. F. Sierra Moreno, "*Modificación de la respuesta óptica de cristales fotónicos de silicio poroso a través de oxidación térmica para aplicaciones ópticas en el UV-VIS*", Tesis doct., 2021.

[34] L. T. Canham, "*Bioactive silicon structure fabrication through nanoetching techniques*", Advanced Materials, vol. 7, n.o 12, pp. 1033-1037, 1995.

[35] B. Allende Sánchez. (2022, March 22)."Modificación de superficies con polidopamina.," p. 71, 2012, [Online]. Available: http://digibuo.uniovi.es/dspace/handle/10651/4162%0Ahttp://digibuo.uniovi.es/dspace/bitstream/10651/4162/1/TFM_Beatriz Allende Sánchez.pdf .

[36] M. Ferrari and L. Canham, "Foreword," in Porous Silicon for Biomedical Applications, H. A. Santos, Ed. Woodhead Publishing, 2014.

[37] R. S. Hebbar, A. M. Isloor, and A. F. Ismail, "*Chapter 12 - Contact Angle Measurements*," in Membrane Characterization, N. Hilal, A. F. Ismail, T. Matsuura, and D. Oatley-Radcliffe, Eds. Elsevier, 2017, pp. 219–255.

[38] (2022, April 30). Espectrometría infrarroja de reflexión-absorción. Universitat Rovira i Virgili. (n.d.). [Online]. Availabe: https://www.urv.cat/es/investigacion/apoyo/recursos-cientificos-tecnicos/serveis/ftir/

[39] (2022, April 30). *Confocal Microscope, Principle & Applications*. Ibidi. 2021. [Online]. Available: https://ibidi.com/content/216-confocal-microscopy.

[40] (2022, Apriol 30). Microscopi Electrònic de Rastreig Ambiental (ESEM). Universitat Rovira i Virgili. (n.d.). [Online]. Available: https://www.urv.cat/es/investigacion/apoyo/recursos-cientificos-tecnicos/serveis/esem/

[41] A.P.F. Turner, I. Karube, G. S. Wilson, "*Biosensors: Fundamentals and Applications*", Oxford University Press, Oxford.p. 770. 2012.

[42] V. González Rumayor, E. García Iglesias, O. Ruiz Galán, and L. Gago Cabezas. (2022, April 10). "Aplicación de biosensores en la industria agroalimentaria," 2005. [Online]. Available: http://hdl.handle.net/20.500.12324/33506 .

[43] A.R. Anandapadmanabhan. (2022, March 10) ."Thesis: Sensins Devices for Illicit Drug Detection". IISER PUNE. [Online]. Available: http://dr.iiserpune.ac.in:8080/xmlui/handle/123456789/766

[44] C. Rivas and B. Dutrenit, "*Uso de biosensores en la práctica médica*," *Univ. ORT Uruguay*, pp. 1–4, 2019.

[45] D. Thévenot, K. Toth, R. Durst, and G. Wils, "*Electrochemical Biosensors: Recommended Definitions and Classifications*," 1999.

[46] N. Elgrishi, K. J. Rountree, B. D. McCarthy, E. S. Rountree, T. T. Eisenhart, and J. L. Dempsey, "*A Practical Beginner's Guide to Cyclic Voltammetry*", *J. Chem. Educ.*, vol. 95, no. 2, pp. 197–206, 2018.

[47] C. Ordóñez. (2022, March 10). Análisis Voltamétrico para la cuantificación de Aciclovir. [Online]. Available: https://repository.icesi.edu.co/biblioteca_digital/bitstream/10906/83023/1/TG01799.pdf

[48] J. G. Osteryoung, R. A. Osteryoung, "*Square Wave Voltammetry*," Anal. Chem., vol. 57, no. 1, pp. 1–6, 1985.

[49] S. Yunus, A. M. Jonas, and B. Lakard, "*Potentiometric Biosensors*," in *Encyclopedia of Biophysics*, G. C. K. Roberts, Ed. Berlin, Heidelberg: Springer Berlin Heidelberg, pp. 1941–1946. 2013.

[50] International Journal, A. Burcu, E. Bahadır, M. Kemal Sezgintürk. Artificial Cells, Nanomedicine, and Biotechnology A review on impedimetric biosensors A review on impedimetric biosensors. *A Review on Impedimetric Biosensors, Artificial Cells*, *44*(1), 248–262. 2016.

[51] N. Jaffrezic-Renault, S. V. Dzyadevych. (2022, April 14). Conductometric Microbiosensors for Environmental Monitoring. *Sensors*, *8*, 2569–2588. 2008. [Online]. Available: www.mdpi.org/sensors .

[52] V. S Lin, K. Motesharei, K. P. Dancil, M. J. Sailor, M. R. Ghadiri. A Porous Silicon-Based Optical Interferometric Biosensor. Science 1997, 278 (5339), 840-843.

[53] L. N. Acquaroli, T. Kuchel, and N. H. Voelcker, "*Towards implantable porous silicon biosensors*", RSC Adv., vol. 4, no. 66, pp. 34768–34773. 2014.

[54] L. M. Bonanno, T. C. Kwong, and L. A. DeLouise, "*Label-Free Porous Silicon Immunosensor for Broad Detection of Opiates in a Blind Clinical Study and Results Comparison to Commercial Analytical Chemistry Techniques*", Anal. Chem., vol. 82, no. 23, pp. 9711–9718, 2010.

[55] C. W. Ferreira, R. Vercauteren, and L. A. Francis, "*Passivated porous silicon membranes and their application to optical biosensing*", *Micromachines*, vol. 13, no. 1, 2022.

[56] N. Reta, A. Michelmore, C. Saint, B. Prieto-Simón, and N. H. Voelcker, "*Porous silicon membrane-modified electrodes for label-free voltammetric detection of MS2 bacteriophage*", Biosens. Bioelectron., vol. 80, pp. 47–53, 2016.